

## Review

# Machine learning interatomic potential: Bridge the gap between small-scale models and realistic device-scale simulations

Guanjie Wang,<sup>1,2</sup> Changrui Wang,<sup>1</sup> Xuanguang Zhang,<sup>1</sup> Zefeng Li,<sup>1</sup> Jian Zhou,<sup>1</sup> and Zhimei Sun<sup>1,\*</sup>

## SUMMARY

**Machine learning interatomic potential (MLIP) overcomes the challenges of high computational costs in density-functional theory and the relatively low accuracy in classical large-scale molecular dynamics, facilitating more efficient and precise simulations in materials research and design. In this review, the current state of the four essential stages of MLIP is discussed, including data generation methods, material structure descriptors, six unique machine learning algorithms, and available software. Furthermore, the applications of MLIP in various fields are investigated, notably in phase-change memory materials, structure searching, material properties predicting, and the pre-trained universal models. Eventually, the future perspectives, consisting of standard datasets, transferability, generalization, and trade-off between accuracy and complexity in MLIPs, are reported.**

## INTRODUCTION

Materials science stands at the forefront of interdisciplinary research, bridging various scientific domains and exploring phenomena across multiple length scales, from atomic to macroscopic.<sup>1–7</sup> The field focuses on how the composition, structure, and processing of materials influence their properties and performance, leading to significant advancements in developing and refining materials.<sup>8,9</sup> The evolution of scientific paradigms from traditional empirical and model-based theoretical approaches to contemporary computational and data-driven methodologies has significantly elevated the role of full-scale simulation in the design and development of materials.<sup>10–16</sup> The primary component of material simulations at any scale is the interatomic potentials, which define the potential energy surfaces (PES) of atomic interactions within a material system.<sup>17–19</sup> These potentials are essential for accurately predicting and understanding the physical and chemical properties of materials, which play a pivotal role not just in materials science, but also in chemistry and condensed matter physics.<sup>20–29</sup> The precise determination of these potentials is crucial for reliable molecular dynamics simulations and studying material behaviors under diverse conditions.<sup>30–47</sup>

Traditionally, interatomic potentials have been derived from empirical methods, while computationally efficient methods often lack the necessary accuracy and transferability for complex systems, such as the embedded-atom method (EAM),<sup>48</sup> empirical N-body potential,<sup>49</sup> Tersoff,<sup>50–52</sup> and so on. First-principles methods, such as Density Functional Theory (DFT), offer higher accuracy but at a significant computational cost, limiting their applicability to smaller systems or shorter timescales.<sup>53,54</sup>

The advent of machine learning (ML) has opened new horizons in the field of interatomic potentials.<sup>55</sup> Machine learning, with its ability to learn from and make predictions or decisions based on data, presents a promising alternative to traditional methods.<sup>56–60</sup> Therefore, Behler and Parrinello proposed an artificial neural network<sup>61</sup> for MLIP with symmetry function descriptors,<sup>62</sup> effectively applied to silicon,<sup>63–65</sup> vinyl bromide,<sup>66</sup> virtual reality,<sup>67</sup> Ge-Te binary compounds,<sup>68</sup> surface diffusion of CO/Ni,<sup>69</sup> Ge-Sb-Te ternary alloys,<sup>70</sup> synthetic chemists,<sup>71</sup> multi-scale-shock dynamics simulations,<sup>72</sup> and many transition-metal oxide compositions.<sup>73,74</sup> Meanwhile, Csanyi et al. also developed the Gaussian approximation potential<sup>75</sup> (GAP) using SOAP descriptors,<sup>76</sup> applied to amorphous carbon<sup>77</sup> and silicon.<sup>78</sup> These two methods now also are the main technologies of MLIPs.<sup>79–94</sup> Previously, there are some review articles on MLIPs, for example, Behler et al.<sup>95–97</sup> outlined the timeline for the evolution of neural network potentials by classifying schemes for MLIPs into four generations; Deringer et al.<sup>98</sup> introduced the basic principles of MLIPs and highlighted the applications to some select problems in materials science, consisting of phase-change materials for memory devices, nanoparticle catalysts, and carbon-based electrodes for chemical sensing, supercapacitors, and batteries; Frieserich et al.<sup>99</sup> summarized the underlying machine learning methods, the data acquisition process and active learning procedures for MLIPs; Unke et al.<sup>100</sup> gave chemical insights into MLIPs and describe a step-by-step guide for constructing and testing them from scratch. In this review article, we highlight the process for constructing MLIPs from the perspective of data, consisting of the high-throughput generation of materials data, conversion of structural data into descriptors, machine learning models for data training, and the application of the

<sup>1</sup>School of Materials Science and Engineering, Beihang University, Beijing 100191, China

<sup>2</sup>School of Integrated Circuit Science and Engineering, Beihang University, Beijing 100191, China

\*Correspondence: zmsun@buaa.edu.cn

<https://doi.org/10.1016/j.isci.2024.109673>



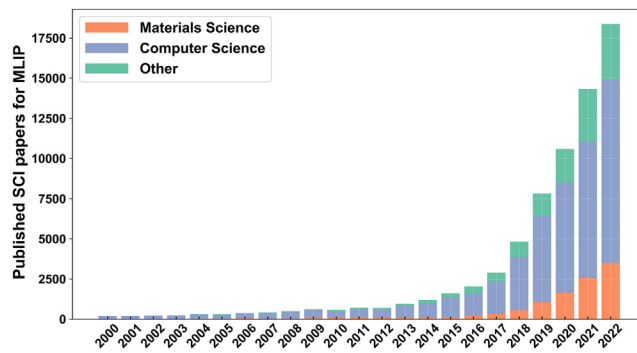


**Figure 1. The number of published scientific articles on the topic of MLIP**

The original data is queried by the keyword of machine learning potential, machine learning force field, and MLIP from Web of Science from 2000 to 2022, as indexed in the Science Citation Index (SCI).

model to new data. In particular, in the model section, we divided the models into six categories based on different ML algorithms and provided executable code for each method.

In detail, this review focuses on the fundamentals, flowcharts, software, applications, and challenges of MLIPs. In section [Fundamental and flowchart of machine learning interatomic potential](#), we introduce the development tendency and the entire key flowcharts related to MLIPs. The data collection methods, material structure descriptor, ML algorithm, and software are presented in sections three to five. The sixth section outlines the application of MLIPs in the selection of phase-change memory materials, structure searching, material properties prediction, and the development of pre-trained universal models. Finally, it looks forward to the challenges and opportunities of MLIPs in the future.

## FUNDAMENTAL AND FLOWCHART OF MACHINE LEARNING INTERATOMIC POTENTIAL

From the year 2000–2022, the number of articles published in MLIP has increased across various fields, as shown in [Figure 1](#). Initially, MLIP research was predominantly rooted in the field of computer science, in which the earliest articles were published.<sup>69</sup> The trend in Computer Science has seen a consistent rise over the years, reflecting the increasing relevance and application of MLIP algorithms in this field.<sup>97</sup> For materials science, there were hardly any MLP publications before 2007. However, there has been a noticeable increment in recent years with the development of supercomputing power and the wave of the AI technology revolution.<sup>101–108</sup>

The training process of machine learning models involves several key steps, as shown in [Figure 2](#). In this part, we focus on introducing the issues that need to be identified at each step.

- Data Collection: the first step is collecting the abundant and necessary data. This involves focusing on the problem to be solved and then gathering all relevant data that can be used to train the model. The data should be as representative as possible of the problem domain and diverse enough to capture all possible conditions.
- Materials Descriptors: once the data is collected, the most important step, which has the greatest impact on the accuracy of the MLIP, is how to convert spatial configurations into a machine learning dataset, also known as the material descriptors. The material descriptor determines the quality of the initial dataset for machine learning and also defines the highest accuracy that the MLIP can achieve. Different machine learning algorithms are merely used to infinitely approximate this optimal goal value. Afterward, several steps such as data cleaning, preprocessing, and normalization are also indispensable. Data cleaning can remove any irrelevant or duplicate data, while preprocessing involves techniques such as scaling or encoding to make the data suitable for training. Normalization is a process of adjusting the data to a common scale for better convergence during training.
- Model Selection: it is essential to choose a model that suits the nature of the problem and has the capacity to learn from the given data. Common models used for MLIP include Gaussian approximation, neural networks, and active learning. Then, it is trained on the prepared data, which involves optimizing the model's parameters using a suitable optimization algorithm such as gradient descent or Adam and so on. The model iteratively updates its parameters based on the feedback provided by the loss function, which measures how well the model is performing on the training data. A crucial aspect of model training is tuning hyperparameter, which are used to control the learning process of the model, such as learning rate, batch size, or the number of hidden layers in a neural network. Common techniques for hyperparameter tuning include grid search, random search, or more advanced methods such as Bayesian optimization or gradient-based optimization. After training, it is essential to evaluate the model's performance on a separate test dataset that was not used during training. This helps in gauging how well the model generalizes to unseen data and provides an accurate estimate of its future performance in real-world scenarios. Evaluation metrics such as accuracy, precision, recall, or F1-score are commonly used to assess the model's performance.
- Model improvement and deployment: based on the evaluation results and feedback from domain experts, further improvements can be made to the model. This might involve modifying the architecture of the model, trying different hyperparameter settings, or incorporating more advanced techniques such as ensemble methods or transfer learning to improve performance. While the model

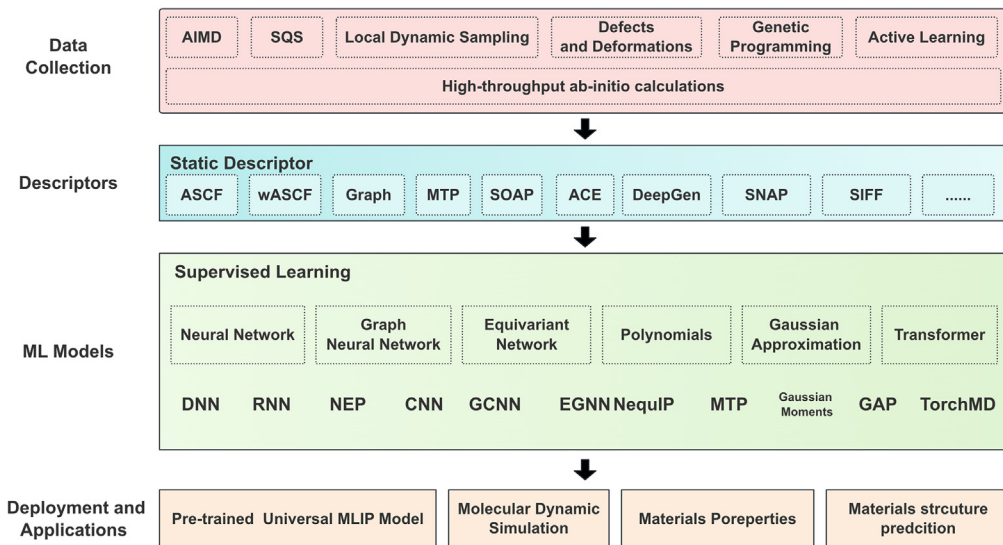


**Figure 2.** The flowchart and four essential stages of MLIPs

achieves satisfactory performance, it can be deployed in a production environment for real-time predictions or decision-making. It is essential to have a well-designed deployment strategy that ensures scalability, fault tolerance, and monitoring of the deployed model's performance over time.

## DATA COLLECTION OF MACHINE LEARNING INTERATOMIC POTENTIALS

Datasets are fundamental to machine learning, providing the raw material from which algorithms learn and derive insights.<sup>109–111</sup> Diverse datasets help in building robust models that can generalize well across different scenarios, reducing biases and improving the accuracy of predictions. In materials science, collecting comprehensive datasets through various methods is vital for exploring the entire spectrum of material properties and behaviors.<sup>112–116</sup> This extensive data collection enables the identification of novel materials with desired characteristics, supports the understanding of complex material interactions, and facilitates the prediction of material performance under different conditions. In this part, we introduce some possible data collection methods for training MLIPs.

- Open-source material databases: the concepts of materials genomics have led to the creation of numerous large-scale materials databases globally, such as ICSD,<sup>117</sup> Materials Project,<sup>118</sup> Aflow,<sup>119</sup> Materials Cloud,<sup>120</sup> NOMAD,<sup>121</sup> ALKEMIE MatterDB,<sup>122–124</sup> OQMAD,<sup>125</sup> COD,<sup>126</sup> OMD,<sup>127</sup> C2DB,<sup>128</sup> MatNavi,<sup>129</sup> among others. These databases provide a wealth of data obtained from DFT calculations, which typically require extensive computational resources. Therefore, efficiently filtering and selecting target materials from these open-source databases presents a highly effective method for gathering relevant data for MLIPs without the need for time-intensive DFT calculations.<sup>130–133</sup>
- Ab Initio Molecular Dynamics (AIMD) Sampling: AIMD simulations to explore the configurational space. The temperature of the simulation determines the regions of the potential energy surface (PES) and energy ranges explored. This technique is suitable for equilibrium or near-equilibrium properties, such as studying vibrational spectra or thermodynamic properties.
- Adaptive Sampling or On-the-Fly ML: this technique starts with a small initial set of reference data to train a preliminary ML potential, which is then used in MD simulations.<sup>134</sup> Additional conformations are collected when model predictions become unreliable, based on an uncertainty criterion, and reference calculations are performed.<sup>135,136</sup>
- Meta dynamics Sampling: similar to adaptive sampling, this method uses preliminary ML potentials in MD simulations but biases the dynamics to visit unexplored regions on the PES.<sup>137–139</sup> It combines metadynamics with uncertainty estimates to select relevant structures.
- Normal Mode Sampling: this approach does not require MD simulations. It starts from a minimum on the PES and generates distorted structures by displacing atoms along normal modes. It is efficient for exploring PES but is limited to regions close to minima and is best combined with other sampling methods.

After collecting data, it is crucial to clean data by feature engineering, including removing inconsistencies, addressing missing values, and filtering out irrelevant information.<sup>140–144</sup> Subsequently, data splitting segregates the refined dataset into training, validation, and test sets, which are used to assess the model's generalization capability while mitigating the risk of overfitting. Concurrently, data standardization and normalization emerge as pivotal steps in preprocessing. Specifically, standardization is the best method to rescale the data to yield a mean of zero and a standard deviation of one, effectively resolving issues arising from differing scales among features. Normalization, often achieved

**Table 1.** The various descriptors list for materials structure

Description	Year	Author
Atom-centered symmetry functions (ACSF)	2011	Behler <sup>62</sup>
Coulomb Matrix	2012	Rupp <sup>152</sup>
Smooth Overlap of Atomic Positions (SOAP)	2013	Csányi <sup>76</sup>
Ewald sum and Sine Matrix	2015	Faber <sup>153</sup>
Spectral neighbor analysis method (SNAP)	2015	Thompson <sup>151</sup>
Moment Tensor Potentials (MTP)	2016	Shapeev <sup>177</sup>
Weighted atom-centered symmetry functions (wACSF)	2018	Gastegger <sup>150</sup>
Automatic selection of fingerprints	2018	Giulio <sup>220</sup>
Atomic-position independent material descriptor (U-api)	2018	Thompson <sup>157</sup>
Deep Potential Dynamic Descriptor (DP)	2018	Zhang <sup>158</sup>
Graph Descriptor	2018	Jeffrey <sup>159</sup>
Optimizing SOAP	2019	Caro <sup>221</sup>
Atomic Cluster Expansion (ACE)	2019	Drautz <sup>156</sup>
Many-body Tensor Representation (MBTR)	2022	Huo <sup>154</sup>

by scaling data within a specific range such as 0 to 1, guarantees that all input features contribute uniformly to model training. In a word, data preprocessing, consisting of feature engineering, data standardization, and normalization, enhances the model's overall performance and stability.<sup>145–149</sup>

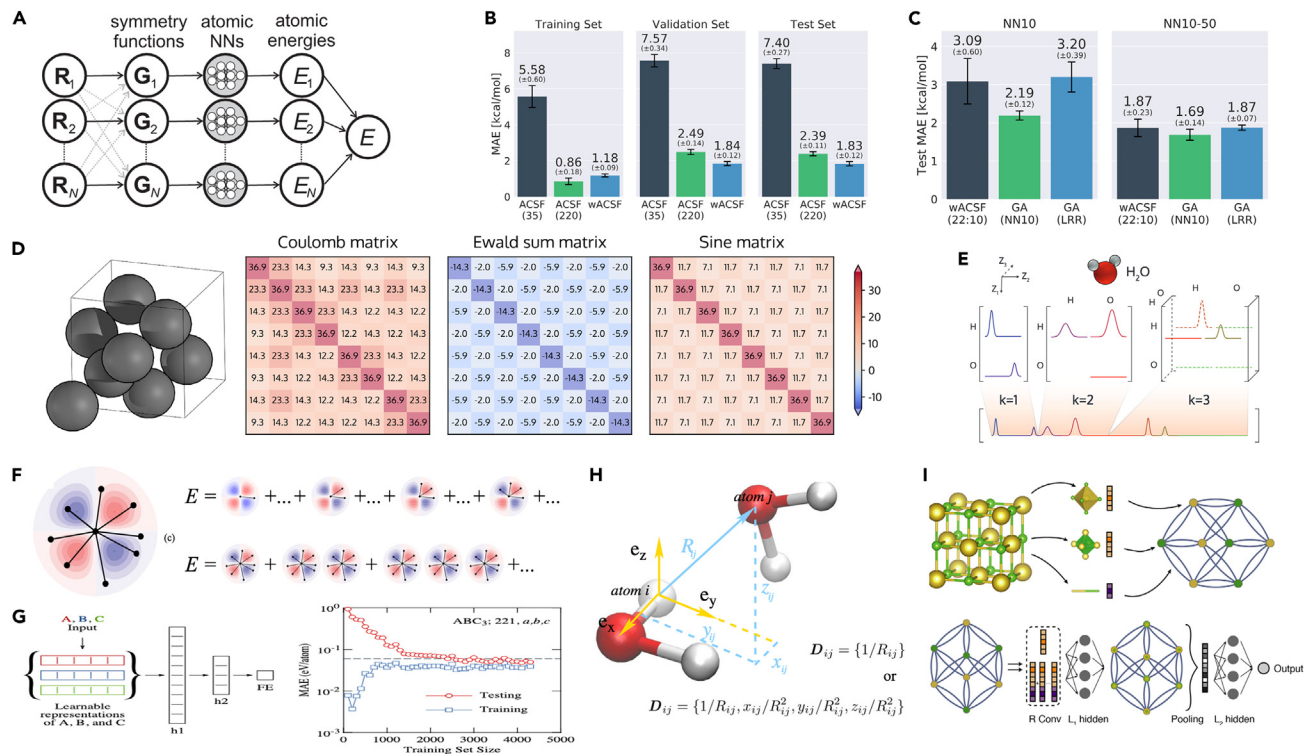
## MATERIALS DESCRIPTORS OF MACHINE LEARNING INTERATOMIC POTENTIALS

To construct an effective descriptor for material structure in MLIP, the following criteria are essential.

- Spatial Translation Invariance: the descriptor must remain consistent regardless of any shifts in the coordinate system, ensuring it respects the isometry of space.
- Rotational Invariance: it should be unaltered by any rotations of the coordinate system, adhering to the principle of isotropy of space.
- Permutation Invariance: the order of atomic indices should not impact the descriptor, meaning that reordering the atoms does not change the system's physical characteristics.
- Uniqueness: each descriptor should be distinctly tied to a specific atomic environment and correspond to a unique property, avoiding multiple representations for the same structure.
- Continuity: the descriptor should sensitively reflect minor variations in atomic arrangements, ensuring a proportional relationship between small structural changes and descriptor adjustments.
- Compactness: while providing comprehensive information necessary for accurate predictions, the descriptor should minimize the number of features to avoid complexity.
- Computational Efficiency: calculating the descriptor should be significantly less resource-intensive compared to direct computations of the physical properties it represents.

Here, we have listed the several commonly used and efficient descriptors, as shown in **Table 1**. In detail, for constructing high-dimensional neural network potentials, Behler<sup>62</sup> first reported atom-centered symmetry functions (ACSF), which can transform cartesian coordinates to a series of symmetry functions to accurately represent atomic environments (**Figure 3A**), and also can be extended to various systems such as molecules, solids, and liquids. Furthermore, Gastegger et al.<sup>150</sup> introduce weighted atom-centered symmetry functions (wACSFs) as an efficient and accurate alternative to conventional atom-centered symmetry functions (ACSFs) for MLIP, which offer better scalability with diverse chemical elements and require fewer functions for equal spatial resolution, significantly improving generalization in machine learning potentials. Utilizing the QM9 database's molecular structures and enthalpies, as shown in **Figures 3B** and **3C**, they demonstrate that wACSFs achieve lower prediction errors compared to ACSFs. Moreover, it shows that simple empirical parametrization schemes are sufficient for high accuracy, and the use of genetic algorithms for optimizing wACSFs can further enhance small neural network potentials.

Nevertheless, Csanyi introduces the Smooth Overlap of Atomic Positions (SOAP) descriptor,<sup>76</sup> which maintains crucial properties such as differentiability with respect to atomic movement and invariance to physical symmetries such as rotation, reflection, translation, and permutation of atoms of the same species, and offers a more faithful representation that remains consistent regardless of the number of neighbors, avoiding the tradeoff between descriptor size and accuracy. This makes SOAP, integrated into GAP software, particularly effective for systems with larger clusters of atoms, where traditional descriptors tend to lose accuracy. Moreover, Thompson et al.<sup>151</sup> introduce the Spectral Neighbor Analysis Potential (SNAP), whose uniqueness lies in its characterization of each atom's local environment through bispectrum components of local neighbor density, projected onto a hyperspherical harmonic basis in four dimensions. Unlike the GAP potential, SNAP

**Figure 3.** Depict of various descriptors

- (A) Atom-centered symmetry functions.<sup>62</sup> (Reproduced with permission from Ref.,<sup>62</sup> © J. Chem. Phys. 2011).
- (B) Weighted atom-centered symmetry functions.<sup>150</sup> (Reproduced with permission from Ref.,<sup>150</sup> © J. Chem. Phys. 2018).
- (C) Weighted atom-centered symmetry functions optimized with the GA using fitness functions based on linear ridge regression and neural network potentials.<sup>150</sup> (Reproduced with permission from Ref.,<sup>150</sup> © J. Chem. Phys. 2018).
- (D) Coulomb, Eward sum and sine matrices.<sup>155</sup> (Reproduced with permission from Ref.,<sup>155</sup> © Comput. Phys. Commun. 2020).
- (E) Many-body tensor representation.<sup>155</sup> (Reproduced with permission from Ref.,<sup>155</sup> © Comput. Phys. Commun. 2020).
- (F) Atomic cluster expansion.<sup>156</sup> (Reproduced with permission from Ref.,<sup>156</sup> © Phys. Rev. B 2019).
- (G) Atomic-position independent material descriptor.<sup>157</sup> (Reproduced with permission from Ref.,<sup>157</sup> © Phys. Rev. B 2018).
- (H) Deep potential dynamic descriptor.<sup>158</sup> (Reproduced with permission from Ref.,<sup>158</sup> © Phys. Rev. Lett. 2018).
- (I) Graph descriptor.<sup>159</sup> (Reproduced with permission from Ref.,<sup>159</sup> © Phys. Rev. Lett. 2018).

assumes a linear relationship between atom energy and bispectrum components, with linear coefficients determined via weighted least-squares linear regression against a comprehensive quantum mechanics training set.

Subsequently, as shown in Figure 3D, Rupp et al.<sup>152</sup> report molecular representation methods based on Coulomb matrices, inspired by the nuclear repulsion term in the molecular Hamiltonian. By transforming the challenge of solving the molecular Schrödinger equation into a more manageable nonlinear statistical regression problem, the model is trained and validated on a dataset of over seven thousand organic molecules, showing a mean absolute error of approximately 10 kcal/mol. This approach demonstrates high accuracy and transferability in predicting atomization energies for a wide range of organic molecules and distorted equilibrium geometries, highlighting the broader utility of the Coulomb matrix as a descriptor in various chemical contexts. Similarly, Faber et al.<sup>153</sup> also generalize the Coulomb matrix representation, successful in modeling atomization energies of organic molecules, to periodic systems using three approaches: (i) a matrix based on the Ewald sum of electrostatic interactions in the unit cell; (ii) an extended Coulomb-like matrix considering neighboring unit cells; and (iii) a sine matrix representation mimicking the periodicity and elemental features of the Ewald sum matrix. These representations were compared using a Laplacian kernel with the Manhattan norm on a dataset of 3938 crystal structures. The generalization error in predicting structure formation energies was 0.49, 0.64, and 0.37 eV/atom for the respective representations. Next, Haoyan et al.<sup>154</sup> highlight the development of a many-body tensor representation (MBTR) for MLIP, which is invariant to translations, rotations, and nuclear permutations, and can represent both molecules and crystals, and is showcased in phase diagrams of Pt-group/transition-metal binary systems, as shown in Figure 3E. The Coulomb, Ewald, sine matrices, and MTBR can be performed in DScripte software packages.<sup>155</sup>

Additionally, Drautz et al.<sup>156</sup> report the atomic cluster expansion (ACE) as a novel and comprehensive descriptor method for MLIP, efficiently scaling linearly with the number of neighbors, a significant improvement over traditional many-atom expansion. Applied to small Cu clusters, it demonstrates smooth convergence to accuracies within the meV range, whose innovation lies in its ability to integrate nonlinear functions into the expansion, producing interatomic potentials that rival the accuracy of advanced MLIPs, as shown in Figure 3F. In addition,

Thompson et al.<sup>157</sup> also report an atomic-position independent material descriptor with the feature of using crystallographic space group and Wyckoff-sites, rather than specific atomic positions, to describe structure details of materials, as shown in Figure 3G. Employing this atomic-position independent descriptor, they also used an attention-weights sharing convolution neural network, which learns across diverse structure types without explicitly using atomic positions, to achieve a mean absolute error of only 0.07 eV/atom in predicting the formation energies of over 85,000 diverse materials.

In addition to the aforementioned static descriptors related to numerical analysis, Zhang et al.<sup>158</sup> have proposed dynamic descriptors in *DeepPotential* software, which involves training a neural network to automatically determine the coefficients of different many-body interaction terms, as shown in Figure 3H. Although this method has improved accuracy, it requires a significant number of computational resources. Particularly, with the development of mathematical graph theory, unlike traditional methods that rely on manually constructed feature vectors or complex transformations of atom coordinates, Jeffrey et al.<sup>159</sup> introduce an original machine learning framework, Crystal Graph Convolutional Neural Networks (CGCNN), which directly learns material properties from the atomic connections within a crystal structure, as shown in Figure 3I. This approach offers a universal and interpretable representation for various types of crystalline materials and has demonstrated high accuracy in predicting properties calculated by DFT for a diverse range of crystal structures and compositions, using a dataset of approximately  $10^4$  data points.

## MACHINE LEARNING MODELS OF MACHINE LEARNING INTERATOMIC POTENTIALS

In this section, we categorize MLIPs into six types of methods and summarize the software codes that can be executed for each type of MLIP, as listed in Table 2. The first type is artificial neural networks (ANN) and deep neural networks (DNN), originally proposed and used in MLIP by Behler et al.,<sup>160</sup> collectively referred to as NN in Table 2. Initially, this model converts spatial configurations into numerical matrices based on the structural descriptors mentioned in Section [Materials descriptors of machine learning interatomic potentials](#), and then iterates the model through forward and backward propagation algorithms, obtaining the best predictive results of the model performance through the loss function, as shown in Figure 3A. Detailed descriptions of this type of model can be found in the referenced articles.<sup>161</sup> This method has now extended to include more single-layer neural network NEP methods, high-dimensional approaches 4G-HDNNP,<sup>97</sup> Accurate Neural Network Engine (ANI-1),<sup>162</sup> Hierarchical Interacting Particle NN,<sup>163</sup> and GPU-accelerated algorithms such as aenet-Pytorch.<sup>164</sup>

The second method is the graph neural network (GNN) model.<sup>159,165–168</sup> The process of constructing a potential function for a graph neural network model in the article can be described as follows, as shown in Figure 4A. The executable code can be found in Table 2.

- Defining relationships between nodes: the relationships between nodes, represented as edges in the graph, are defined. In the context of chemical molecules, nodes can represent atoms, and edges can represent chemical bonds. The similarity between nodes is also determined.
- Establishing graph convolutional network: the core of the graph neural network is the graph convolutional network, which models the relationships between nodes. Parameters such as the number of layers, the number of nodes per layer, and the feature dimensions of the nodes are determined. Additionally, the similarity calculation and weight update methods between nodes are specified.
- Extracting node features: each node in the graph convolutional network has a set of feature vectors representing its attributes. These feature vectors undergo nonlinear transformations to extract and transform more meaningful representations. The parameters for the nonlinear transformation and the dimensions of the feature vectors are determined.
- Training and optimizing the model: the potential function represents the state or behavior of the nodes in the graph neural network. It calculates the output value for each node. After defining the potential function, the model is trained and optimized using training data. Gradient descent or other optimization algorithms are employed to update the model's parameters, enhancing its prediction accuracy. Hyperparameters, loss functions, and evaluation metrics for the model are also determined during this process.

Furthermore, message passing network is one type of GNN, rapidly advancing in accuracy and generality for MLIPs. This research presents a TensorMol-0.1 model,<sup>169</sup> which describes an original approach to energy calculation using a combination of short-range and long-range potentials based on message-passing neural networks. A key feature is the use of TensorFlow for automatic differentiation in molecular potential calculations, allowing for the efficient optimization of network weights. The study also introduces a charge model for molecular dipole moments and a modified damped-shifted force for Coulomb energy calculation, ensuring smooth transition and differentiability, as shown in Figure 4B. The other message passing GNN include DimeNet++,<sup>170</sup> DimeNet,<sup>171</sup> MACE,<sup>172</sup> and so forth.

Next, the third method of MLIPs is the E(n)-Equivariant Graph Neural Networks (EGNNs),<sup>173</sup> an original model for learning graph neural networks that are equivariant to rotations, translations, reflections, and permutations, as shown in Figure 4C. Unlike existing methods, the EGNNs do not require computationally intensive higher-order representations in intermediate layers, yet they deliver competitive or superior performance. A distinctive advantage of the EGNNs is their scalability to higher-dimensional spaces beyond the typical 3D, broadening their applicability. The article demonstrates the model's effectiveness in various applications including dynamical systems modeling, graph autoencoder representation learning, and predicting molecular properties. In the same way, there are many other EGNN models, such as NequIP,<sup>174</sup> UNET,<sup>175</sup> Tensor-Field Networks,<sup>176</sup> and so forth.

As shown in Figure 4D, the fourth category of MLIPs is polynomial-type,<sup>177</sup> which are potential function fitting methods formed by combinations of polynomials, similar to the MTP descriptors and others mentioned in the descriptor in Section [Materials descriptors of machine learning interatomic potentials](#). The fifth MLIP is Gaussian Approximation Potential,<sup>75</sup> which addresses the gap between models that explicitly treat electrons and those that do not, aiming to accurately model the Born-Oppenheimer potential energy surface (PES) without simulating

**Table 2.** The list of implemented software of various MLIP models

Model	Type	Release time	Reference
NNP	NN	1995	Blank <sup>69</sup>
BPNN	NN	2007	Behler <sup>160</sup>
ænet-Fortran	NN	2016	Artrith <sup>222</sup>
DTNN	NN	2017	Schutt <sup>223</sup>
ANI-1	NN	2017	Smith <sup>162</sup>
HIP-NN	NN	2018	Nebgen <sup>163</sup>
SchNet	NN	2018	Schutt <sup>224</sup>
DeepPotential	NN	2018	Zhang <sup>158,225,226</sup>
PhysNet	NN	2019	Unke <sup>227</sup>
ACE	NN	2019	Drautz <sup>156</sup>
LieConv	NN	2020	Finzi <sup>228</sup>
4G-HDNNP	NN	2021	Ko <sup>97</sup>
NEP	NN	2021	Fan <sup>229</sup>
ænet-Pytorch	NN	2023	Artrith <sup>164</sup>
GNNFF	GraphNN	2021	Park <sup>230</sup>
MDGNN	GraphNN	2021	Wang <sup>231</sup>
NoisyNodes	GraphNN	2022	Godwin <sup>232</sup>
M3GNet	GraphNN	2022	Chen <sup>211</sup>
TeaNet	GraphNN	2022	Takamoto <sup>233</sup>
PotentialMind	GraphNN	2023	Wang <sup>187</sup>
CHGNet	GraphNN	2023	Deng <sup>214</sup>
TensorMol 0.1	GraphNN	2018	Yao <sup>169</sup>
DimeNet++	GraphNN	2020	Gasteiger <sup>170</sup>
DimeNet	GraphNN	2020	Gasteiger <sup>171</sup>
NewtonNet	GraphNN	2021	Haghhighatlari <sup>234</sup>
SphereNet	GraphNN	2021	Liu <sup>235</sup>
PAINN	GraphNN	2021	Schutt <sup>236</sup>
GemNet	GraphNN	2022	Gasteiger <sup>237</sup>
HermNet	GraphNN	2022	Wang <sup>238</sup>
MACE	GraphNN	2022	Batatia <sup>172</sup>
Allegro	GraphNN	2023	Musaelian <sup>239</sup>
Tensor-Field	EquivariantNetwork	2018	Thomas <sup>176</sup>
Cormorant	EquivariantNetwork	2019	Anderson <sup>240</sup>
UNET	EquivariantNetwork	2021	Qiao <sup>175</sup>
EGNN	EquivariantNetwork	2021	Satorras <sup>173</sup>
NequIP	EquivariantNetwork	2022	Batzner <sup>174</sup>
MTP	Polynomials	2016	Shapeev <sup>177</sup>
IPMLs	Polynomials	2018	Bereau <sup>241</sup>
aPIPs	Polynomials	2021	Allen <sup>242</sup>
GAP	Gaussian	2010	Bartok <sup>75</sup>
FCHL19	Gaussian	2020	Christensen <sup>178</sup>
GMNN	Gaussian	2020	Zaverkin <sup>179</sup>
SE(3)-Transformers	Transfomer	2020	Fuchs <sup>243</sup>
DeepMoleNet	Transfomer	2021	Liu <sup>244</sup>
TorchMD-NET	Transfomer	2022	Thölke <sup>180</sup>

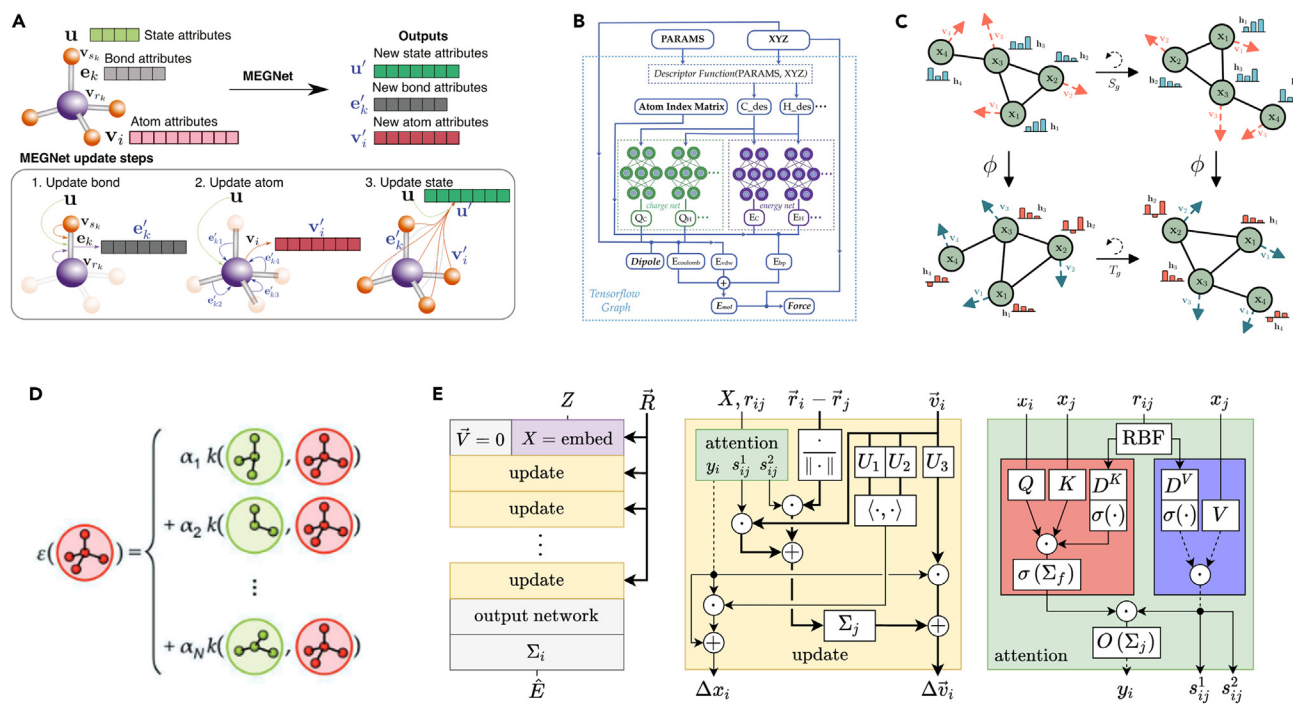


**Figure 4. Schematic of the ML model in MLIPs**

- (A) Many-body graph potential and the major computational blocks.<sup>165</sup> (Reproduced with permission from Ref.,<sup>165</sup> © Chem. Mater. 2019).
- (B) Charge the network and energy network for message passing network.<sup>169</sup> (Reproduced with permission from Ref.,<sup>169</sup> © Chem. Sci. 2018).
- (C) Example of rotation equivariance on a graph.<sup>173</sup> (Reproduced with permission from Ref.,<sup>173</sup> © Int. Conf. Mach. Learn. 2022).
- (D) Polynomial model.<sup>98</sup> (Reproduced with permission from Ref.,<sup>98</sup> © Adv. Mater. 2019).
- (E) Transformer model.<sup>180</sup> (Reproduced with permission from Ref.,<sup>180</sup> © The Author(s). 2022).

electrons, such as FCHL19,<sup>178</sup> GMNN,<sup>179</sup> and so forth. Finally, this study introduces TorchMD-NET,<sup>180</sup> a novel equivariant Transformer (ET) architecture for MLIP, notably overcoming the traditional trade-off between accuracy and computational speed. The model sets a standard in accuracy and efficiency, outperforming existing methods on the MD17, ANI-1, and QM9 datasets. A key feature of TorchMD-NET is its attention-based architecture that leverages rotationally equivariant features, making it particularly effective in predicting energies and atomic forces in molecular dynamics. The study also emphasizes the importance of including off-equilibrium conformations in training datasets for a more accurate evaluation of molecular potentials. By analyzing the model's attention weights, the researchers gain insights into the molecular representation, noting differences in how the model treats hydrogen atoms in energy-minimized molecules versus those in off-equilibrium states, as shown in Figure 4E.

## APPLICATION OF MACHINE LEARNING INTERATOMIC POTENTIALS IN MATERIALS SCIENCE

### Accelerating the molecular dynamic calculation in multi-scale simulation

Gabriele<sup>61</sup> firstly reports the creation and validation of a Neural Network (NN) potential for the phase change materials (PCMs) GeTe. The NN potential successfully replicates the characteristics of GeTe's crystalline, liquids, and amorphous states, closely matching previous DFT calculations, as shown in Figure 5A. The study highlights the potential's robustness in larger (4096-atom) simulations and its sensitivity to fluctuations in smaller (216-atom) models. Notably, the NN potential is also applicable to slightly altered GeTe alloys but faces limitations with off-stoichiometric compositions, such as Ge<sub>0.15</sub>Te<sub>0.85</sub>, due to its inability to accurately model long Te-Te chains.<sup>181–183</sup> Additionally, using the GAP framework, another research<sup>184</sup> introduces an MLIP for the single ternary PCMs compounds of Ge<sub>2</sub>Sb<sub>2</sub>Te<sub>5</sub>, which enabled the creation of a detailed 7200-atom model, providing insights into the material's structure, and facilitated the generation of smaller models for in-depth chemical bonding studies, as shown in Figure 5B. Furthermore, without extra datasets, they expand the above model to six Sb-Te alloy PCMs,<sup>185,186</sup> with compositions ranging from 2:3 to 4:1, revealing that all exhibit similar local structural motifs of defective octahedra. Figure 5C reveals that the crystallization behavior can be influenced by the noticeable shift in medium-range order and cavity concentration with the Sb content increases. For instance, Sb<sub>2</sub>Te<sub>3</sub>, fulling of ABAB rings, favors nucleation-driven crystallization, while Sb-rich alloys such as Sb<sub>4</sub>Te show more 5-fold rings, leading to growth-driven crystallization due to structural dissimilarities with the crystalline phase. Meanwhile, Wang et al.<sup>187</sup> also develop a graph convolution neural network for six binary Sb-Te alloys, with a broader composition ranging from 7:1 to 1:2, as shown in Figure 5D. For the exploration of PCM behaviors in realistic memory device geometries and conditions, Zhou et al.<sup>30</sup> introduce an ML-based potential model, trained using quantum-mechanical data, to simulate all Ge-Sb-Te compositions used in PCMs, which significantly enhances

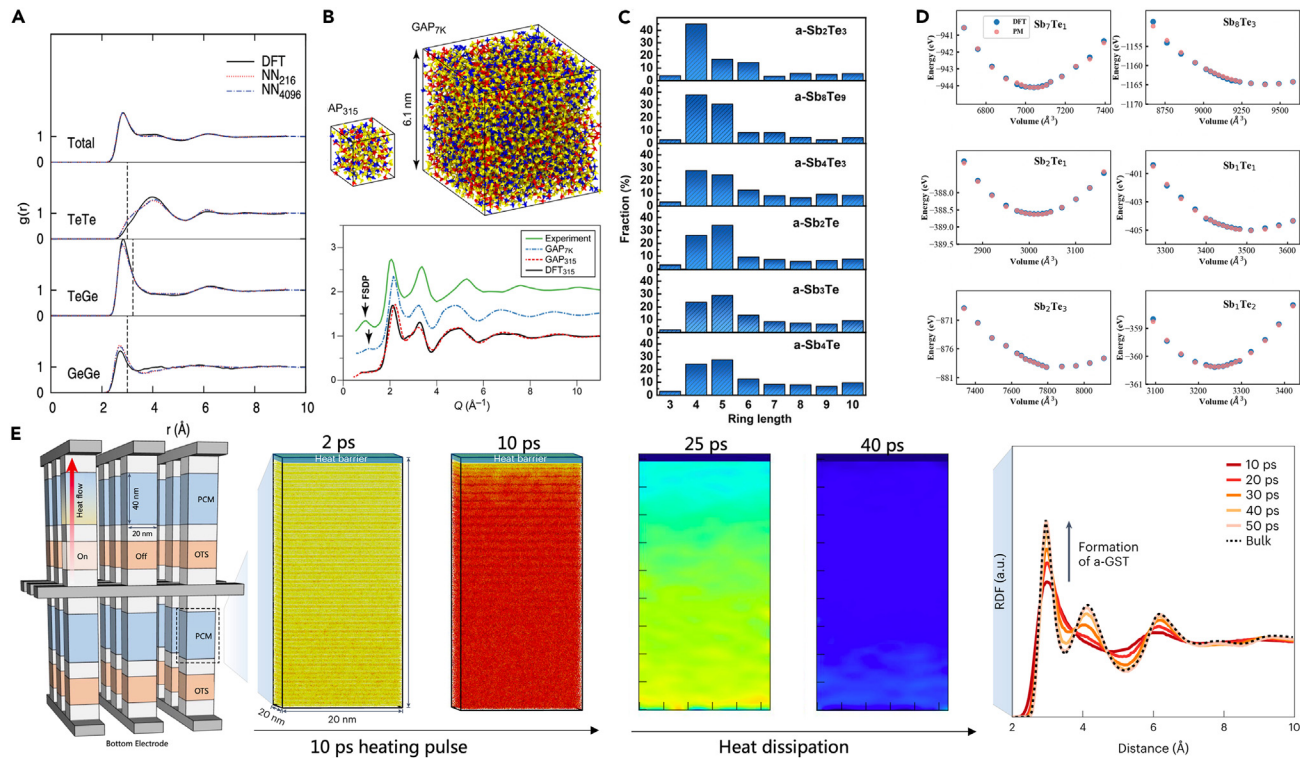


**Figure 5. The molecular dynamic calculation results, which is accelerated by MLIPs in multi-scale simulation**

- (A) The radial distribution function compared MLIP with DFT in GeTe.<sup>61</sup> (Reproduced with permission from Ref.,<sup>61</sup> © Phys. Rev. B 2012).
- (B) The radial distribution function compared MLIP with DFT in Ge<sub>2</sub>Sb<sub>2</sub>Te<sub>5</sub>.<sup>184</sup> (Reproduced with permission from Ref.,<sup>184</sup> © J. Phys. Chem. B 2018).
- (C) The fraction of primitive rings for the six amorphous Sb-Te alloys.<sup>185</sup> (Reproduced with permission from Ref.,<sup>185</sup> © Phys. Status Solidi Rrl: Rapid Res. Lett. 2021).
- (D) The energy-volume curves of six crystal Sb-Te alloys.<sup>187</sup> (Reproduced with permission from Ref.,<sup>187</sup> © J. Phys. Chem. C 2023).
- (E) Schematic of commercial cross-point products, the processes of melting and heat dissipation in a Ge<sub>1</sub>Sb<sub>2</sub>Te<sub>4</sub> structural model, and the evolution of the amorphous GST.<sup>219</sup> (Reproduced with permission from Ref.,<sup>219</sup> © Sci. Bull. 2023).

the speed and accuracy of atomistic simulations. Notably, it supports simulations of multiple thermal cycles and operations crucial for neuro-inspired computing, including cumulative SET and iterative RESET processes. A large-scale device model, containing over half a million atoms, demonstrates the model's capability to accurately depict critical processes in PCM-based memory devices, as shown in Figure 5E. Since the scaling of MLIPs with  $O(N_{\text{electron}})$  is identical to that of a traditional force-field MD simulation, compared with the  $O(N_{\text{electron}}^3)$  scaling of DFT, this cost reduction is more effective for multi-scale simulation. Based on data from experiments and *ab initio* calculations as references, Rowe et al.<sup>188</sup> developed a GAP MLIPs model to simulate the thermal expansion of graphene, detailing the spread of small molecules on graphene surfaces and addressing nuclear quantum effects through path integral molecular dynamics, which is especially useful when precise descriptions of processes are required. MLIPs have also been used in actinide molten salts in nuclear energy. For instance, Nguyen<sup>189</sup> developed an MLIP model using AIMD data with 90 atoms, which enables the acquisition of extended molecular dynamics trajectories (in nanoseconds) for larger systems ( $10^3$  atoms) at significantly reduced computational cost, facilitating the exploration of bonding structures, thermodynamics, and dynamics across various temperatures. Deng et al.<sup>190</sup> expended MLIPs on complex ceramics with three kinds of representative structures, i.e., Ti<sub>3</sub>SiC<sub>2</sub> of the MAX structure, zircon of the mineral structure, and lead zirconate titanate of the perovskite structure, facilitating the analysis and design of complex crystalline materials. Miwa et al.<sup>191</sup> successfully applied MLIPs for large molecular dynamics simulations of the lithium superionic conductor Li<sub>10</sub>GeP<sub>2</sub>S<sub>12</sub>. In a word, MLIPs offer an accuracy nearly equivalent to that of AIMD but at a much lower cost, which accelerates molecular dynamic calculations for large material systems (up to 100 million atoms<sup>192</sup>), bridging the gap in multi-scale simulation.

### Prediction of material properties

MLIP has been widely applied to predict various material properties. For metal alloys, a study has developed a MTPs approach<sup>193</sup> for materials prediction using MLIP to approximate quantum-mechanical energies, coupled with an active learning algorithm for optimal training dataset selection. Unlike methods limited to a few lattice types, this approach can predict structures with lattice types absent in the training dataset. For Cu-Pd, Co-Nb-V, and Al-Ni-Ti metallic alloys, they discovered stable structures beyond AFLOW's listings, thanks to exploring a vast number of candidate structures (40,000 for Cu-Pd, 27,000 for Co-Nb-V, and 377,000 for Al-Ni-Ti) and using MTPs for relaxation. This method drastically cuts

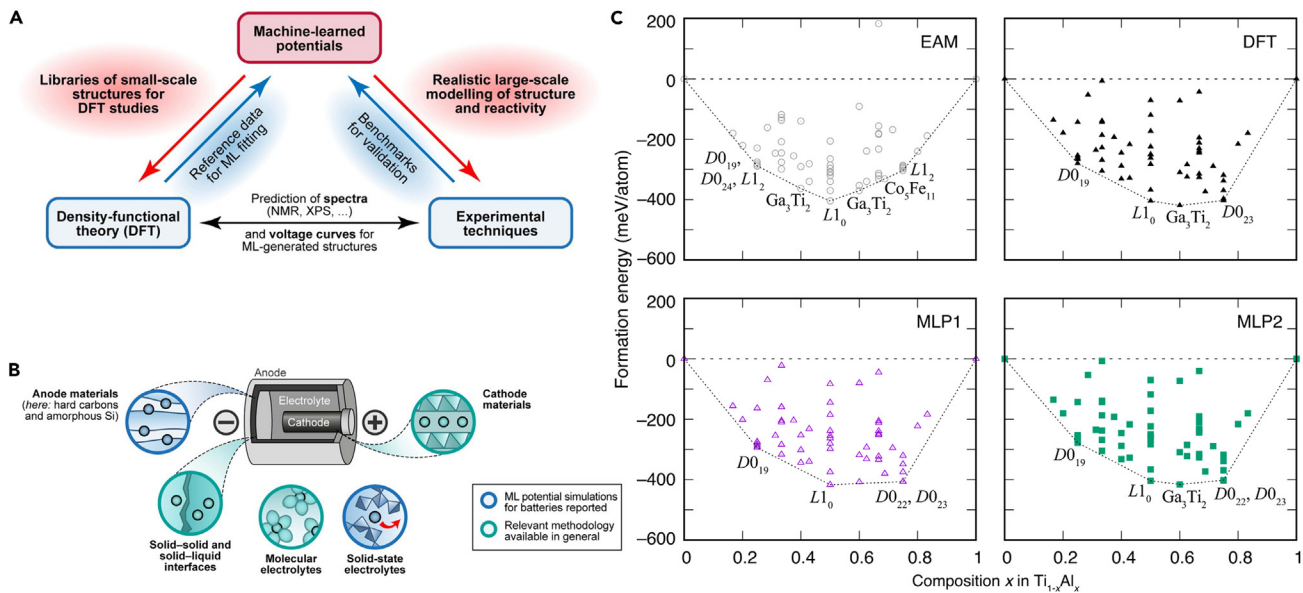


**Figure 6. The flowcharts and results of the application of MLIPs in the prediction of material properties**

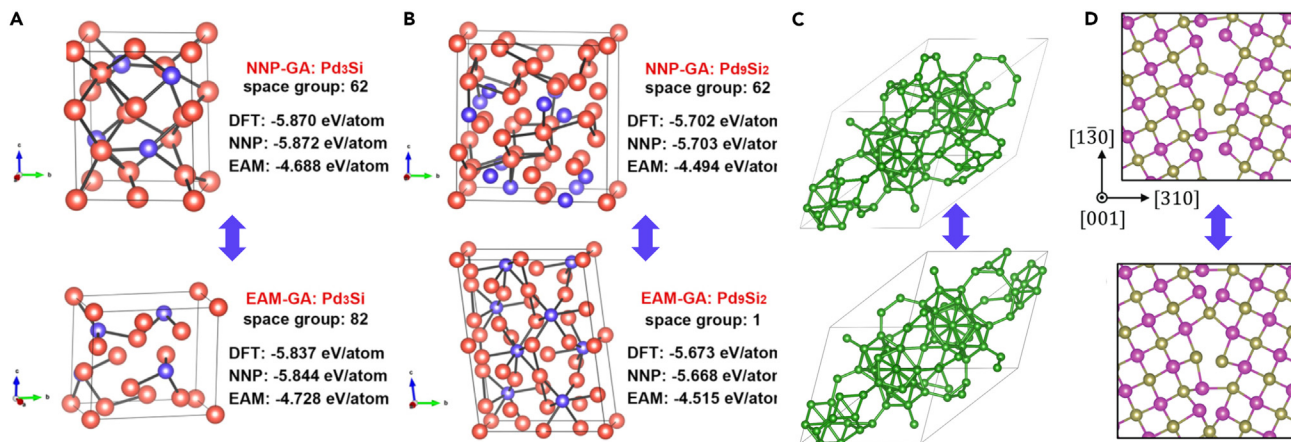
(A) A viewpoint on the synergy between machine learning-based potentials, traditional density functional theory (DFT) methods, and experimental approaches in pursuing the characterization and comprehension of battery materials at the atomic level.<sup>195</sup> (Reproduced with permission from Ref.,<sup>195</sup> © J. Phys. Energy 2020). (B) A highly simplified sketch of different components of a battery, each requiring different atomistic modeling approaches.<sup>195</sup> (Reproduced with permission from Ref.,<sup>195</sup> © J. Phys. Energy 2020).

(C) Formation energies and convex hull of Ti<sub>10</sub>xAl<sub>x</sub> with different compositions.<sup>198</sup> (Reproduced with permission from Ref.,<sup>198</sup> © Phys. Rev. B 2020).

down on the number of required DFT calculations, marking a significant advancement in the discovery of alloy phases, especially for those with multiple components. For studying phononic properties of materials,<sup>194</sup> particularly focusing on low-symmetry and 2D nanomaterials. Bohayra et al. have developed an MLIP method as an efficient alternative to the traditional DFT simulations with PHONOPY code, which often face high computational demands and can produce nonphysical results for such complex structures. This study demonstrate that this approach can accurately and efficiently substitute traditional DFT methods, offering a practical solution for assessing the dynamical stability and phononic properties of complex materials. In addition, MLIP serves as a pivotal tool, complementing established DFT methods and experimental techniques, particularly in characterizing and understanding battery materials at an atomic scale,<sup>195,196</sup> as shown in Figure 6A. This integration of ML-based potentials with traditional approaches enhances our capability to delve into the complex nature of battery components. The utilization of ML-based potentials is especially crucial given the diverse atomistic modeling requirements of different battery components, as illustrated in a simplified sketch of a battery's various parts in Figure 6B. This development marks a stride forward in the precision and efficiency of modeling battery materials, providing a more comprehensive understanding of their atomic-level behavior and interactions.

As shown in Figure 6C, for the prediction of mechanical properties, MLIPs are used to predict the elastic constants and mechanically induced rippling in graphene and hBN,<sup>197</sup> stacking fault energy of Ti-Al alloys,<sup>198</sup> elastic tensor of C<sub>11</sub>, C<sub>21</sub>, and C<sub>44</sub>, and dislocation emissions of Al-Cu alloys.<sup>199</sup> For instance, Arabha et al.<sup>200</sup> highlight the application of MLIPs for assessing the mechanical properties of nitrogenated holey graphene (C<sub>2</sub>N), a two-dimensional nanomaterial. They revealed a thermal conductivity of 85.5 ± 3 W/m-K and an elastic modulus of 390 ± 3 GPa, demonstrating close agreement with DFT results. Additionally, their study explored the impact of point defects on C<sub>2</sub>N's mechanical properties, showing a reduction in the elastic modulus, fractural stress, and ultimate strength with the incorporation of defects. The effectiveness of MLIPs in simulating the thermal and mechanical behavior of C<sub>2</sub>N, including defective structures, underscores their potential as a powerful tool for predicting the properties of two-dimensional nanostructures. By developing a model named UNEP-v1, Fan et al.<sup>201</sup> constructed unified general MLIPs for 16 elemental metals and their alloys, showing an efficient approach to represent the vast chemical space without the need to generate training data for all possible combinations. This work highlights the MLP's application in investigating the mechanical behavior of complex materials, such as the plasticity and primary radiation damage in MoTaVW refractory high-entropy alloys. The study's approach, which employs distinct neural networks for each species and multiple loss functions for parameter optimization, is scalable and adaptable, paving the way for future models that could encompass the entire periodic table.

In addition to their strong potential in simulating and assessing mechanical properties, MLIPs have also been shown to predict characteristics of thermal properties effectively. Arabha et al.<sup>200</sup> reviewed the thermal conductivity of a few 2D and 3D structures, which have been calculated using MLIPs, and compared with their experimental and quantum counterparts. Ladygin et al.<sup>202</sup> introduced a groundbreaking method integrating active learning and MLIPs, specifically moment tensor potentials (MTPs), for predicting lattice dynamics properties with accuracy comparable to DFT. The research thoroughly evaluated the accuracy of these potentials by investigating four materials (Al, Mo, Ti, and U) with varying phonon and thermodynamic properties, achieving high fidelity in reproducing both harmonic and anharmonic

**Figure 7. Comparison of the structure searching results by DFT and MLIPs**

Lowest-energy structures obtained from the classical GA searches by NNP and EAM at the composition of (A) Pd<sub>3</sub>Si and (B) Pd<sub>9</sub>Si<sub>2</sub> with the corresponding DFT, NNP, and EAM energies.<sup>206</sup> (Reproduced with permission from Ref.,<sup>206</sup> © Phys. Rev. B 2019).

(C) Comparison of the found 106-atom structure and the existing structure.<sup>207</sup> (Reproduced with permission from Ref.,<sup>207</sup> © Phys. Rev. B 2019).

(D) Grain boundary structures predicted by ANN and DFT structural relaxation.<sup>209</sup> (Reproduced with permission from Ref.,<sup>209</sup> © Phys. Chem. Chem. Phys. 2022).

behaviors. Furthermore, the study showcases the MLIPs' capability to efficiently calculate phonon dispersion curves and vibrational density of states, providing insights into materials' thermodynamic performances. Notably, MLIPs offer substantial computational speed-ups over traditional DFT calculations without compromising accuracy, marking a significant advancement in the field of materials science and enabling detailed exploration of complex material behaviors on an unprecedented scale. In addition, MLIPs are used for predicting the phonon density of states for  $\beta$ -Ga<sub>2</sub>O<sub>3</sub> consisting of 2500-atoms,<sup>203</sup> unraveling the significant regulation of stress on the contribution of optical phonons to thermal conductivity in layered Li<sub>2</sub>ZrCl<sub>6</sub>,<sup>204</sup> exploring the four-phonon scattering in WS<sub>2</sub>,<sup>205</sup> to name a few.

### Structure searching

In materials science, the conventional approach of calculating material energies through DFT is widely adopted due to its high accuracy. However, a significant drawback of DFT is its time-consuming nature, particularly in the structural search of complex material systems. To overcome this limitation, MLIP methods leverage machine learning techniques to predict material properties and energies, significantly speeding up the structure search process while maintaining reasonable accuracy. By learning from existing DFT computational data, these methods rapidly evaluate a vast array of potential material structures, greatly enhancing the efficiency of material design and discovery. Recent research highlights the development of neural network MLIP for the Pd-Si system,<sup>206</sup> addressing the challenge of achieving both accuracy and efficiency in structure prediction. The NNP methods demonstrate superior accuracy over the existing embedded-atom method (EAM) potential, especially in predicting ground-state structures for Pd<sub>3</sub>Si and Pd<sub>9</sub>Si<sub>2</sub> compositions, where the EAM potential fails, as shown in Figure 7A. Additionally, Evgeny et al.<sup>207</sup> introduces a crystal structure prediction methodology combining the evolutionary algorithm USPEX with an MLIP that learns on-the-fly, which significantly accelerates the process, offering a computational efficiency several orders of magnitude greater than DFT methods. It automates the construction of the interatomic interaction model, eliminating the need for manual training dataset assembly and seamlessly replacing DFT in the prediction algorithm. Tested on various elements including carbon, sodium under high pressure, and boron, as shown in Figure 7B. In order to predict grain boundary, Takayuki et al.<sup>208,209</sup> highlight the effectiveness of MLIP in predicting grain boundary energies in face-centered-cubic (fcc) elemental metals such as Ag, Al, Au, Cu, Pd, and Pt. Despite the absence of grain boundary structures in the training datasets, MLIPs demonstrated high accuracy in forecasting grain boundary structures and energies, aligning well with DFT. Furthermore, Tatsuya et al. present the development of an artificial neural network (ANN) MLIP for accurately predicting grain boundary (GB) atomic structures in CdTe. Using a comprehensive training dataset that includes DFT data of point defects, surfaces, and GBs, the ANN potential was trained to cover various atomic environments. The potential's effectiveness was demonstrated by its ability to predict low-energy structures and GB energetics with accuracy comparable to DFT results, outperforming conventional empirical potentials, as shown in Figure 7C. The study also outlines a method for improving the ANN potential's transferability to more complex GBs, using limited training data. Except for predicting grain boundary configurations, MLIP methods for predicting crystal defects have also been developed. As shown in Figure 7D, Alexandra et al. introduce a novel quadratic noise ML (QNML) approach for bcc Fe and W, focusing on accurately modeling radiation defects and dislocations, enhancing the accuracy of standard linear MLIP without compromising transferability. These potentials, trained on a range of defect configurations, accurately predict complex issues such as the stability and mobility of defects, which is challenging for semiempirical potentials.

### Pre-trained universal machine learning interatomic potential model

Existing MLIPs are generally designed for narrow target materials, making them unsuitable for broader applications in material discovery. Therefore, Takamoto et al.<sup>210</sup> first report PreFered Potential (PFP), a universal Neural Network Potential (NNP) capable of handling any

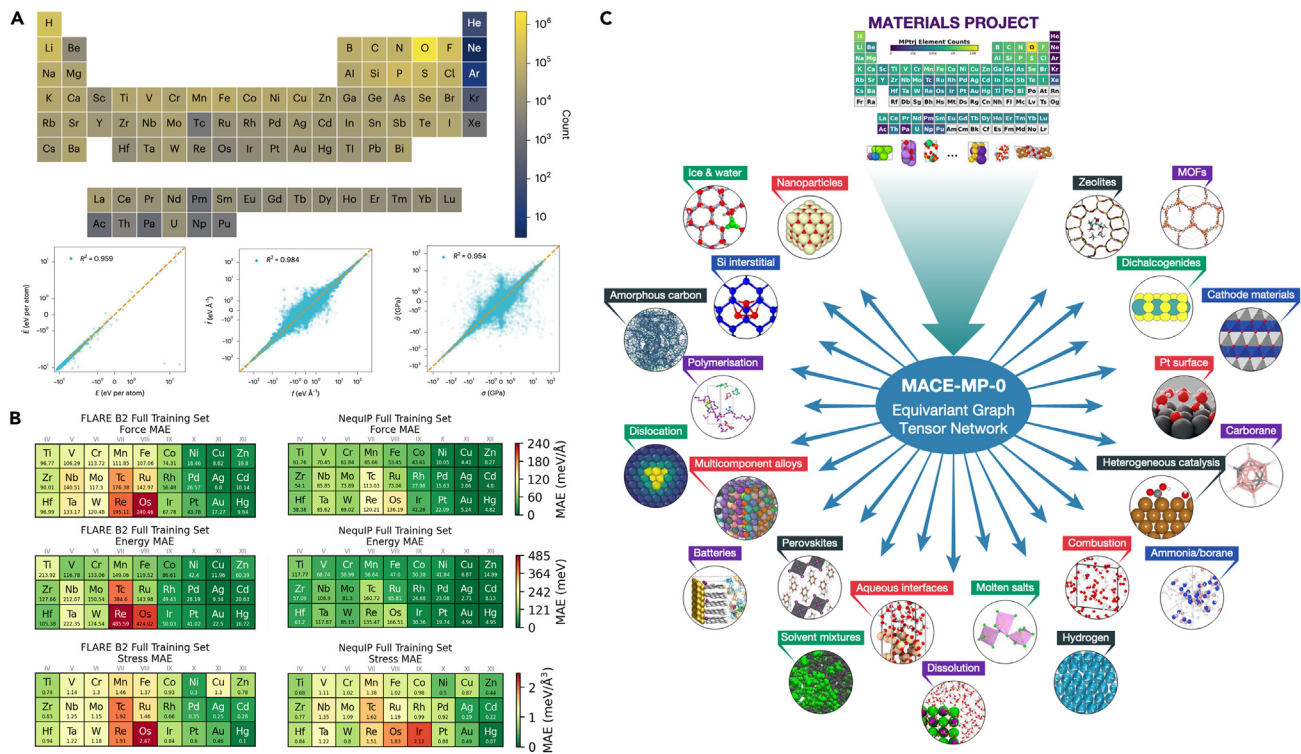


**Figure 8. The three pre-trained universal MLIPs model**

(A) Element counts for all atoms in the dataset, covering 89 elements across the periodic table. And the model predictions on the test dataset compared to DFT calculations.<sup>211</sup> (Reproduced with permission from Ref.,<sup>211</sup> © Nat. Comput. Sci. 2022).

(B) Force, energy, and stress mean absolute errors for the 27 TM systems, using the B<sub>2</sub> invariant ACE descriptors and NequIP.<sup>212</sup> (Reproduced with permission from Ref.,<sup>212</sup> © The Author(s). 2023).

(C) A foundation model for materials modeling, which is based on Materials Project data. MACE-MP-0 is capable of molecular dynamics simulation across a wide variety of chemistries in the solid, liquid, and gaseous phases.<sup>213</sup> (Reproduced with permission from Ref.,<sup>213</sup> © The Author(s). 2023).

combination of 45 elements. Unlike existing NNPs tailored for specific materials, PFP's versatility is demonstrated in diverse applications, including lithium diffusion in LiFeSO<sub>4</sub>F, molecular adsorption in metal-organic frameworks, Cu-Au alloy transitions, and Fischer-Tropsch catalyst discovery. PFP shows high quantitative accuracy and computational efficiency, even reproducing structures and properties not initially considered in its design.

In addition, Shyue et al.<sup>211</sup> introduce a universal MLIP model (M3GNet) based on graph neural networks with three-body interactions, trained on the extensive Materials Project database. M3GNet can be applied to a wide range of materials for structural relaxation, dynamic simulations, and property prediction. Figure 8A reveals the distribution of the initial datasets and the accuracy on the test dataset compared to DFT calculations. Using M3GNet, around 1.8 million potentially stable materials were identified from 31 million hypothetical structures, with 1,578 out of the top 2,000 low-energy materials confirmed as stable via DFT. M3GNet's broad applicability extends to molecular dynamics simulations, identifying potential lithium superionic conductors and serving as a surrogate for DFT in other structural exploration techniques. Its current version, the best achievable with existing data, anticipates future enhancements through more accurate training data and active learning strategies.

For many-body interactions, recent research focuses on the accuracy of MLIPs for bulk solid and liquid phases of d-block elements (TM23 dataset).<sup>212</sup> It compares two FLARE and NequIP models in transition metals, revealing that early transition metals pose a greater challenge in learning accuracy than later group metals, as shown in Figure 8B. The complexity of interatomic interactions varies among these metals, influenced by their electronic structures and the many-body character of interactions. Additionally, based on 1.5 million structures dataset, Ceder et al. also trained a universal graph MLIP, named Crystal Hamiltonian Graph Neural Network (CHGNet), to learn and accurately represent the orbital occupancy of electrons, enhancing its capability to describe both atomic and electronic degrees of freedom.

Another work introduces MACE-MP-0,<sup>213</sup> as shown in Figure 8C, a general-purpose machine-learned force field model, trained on a public database of 150k inorganic crystals. Capable of stable molecular dynamics across various materials, MACE-MP-0 marks a significant advancement in atomistic modeling, demonstrating both qualitative and quantitative accuracy in diverse physical science problems, including water and aqueous systems, catalysis, metal-organic frameworks and the performance on calculating phonon dispersions, bulk and shear moduli of crystals, atomic energies and lattice constants of elemental solids, the cohesive energies of molecular crystals, the reaction barrier heights, and the homonuclear diatomic binding curves. Despite its broad applicability, the model has limitations, including its reliance on the PBE

exchange-correlation functional, lack of explicit long-range interactions, and challenges in capturing intermolecular interactions and high-pressure conditions. Future improvements may involve refitting with modern functionals, incorporating electrostatic and spin interactions, and extending training data. MACE-MP-0, while a foundational model, still requires fine-tuning for specific systems, but shows promise as a step toward democratizing MLIP by lowering barriers to entry in material simulations.<sup>214</sup>

## PERSPECTIVE OF MACHINE LEARNING POTENTIAL

### Standard datasets for machine learning interatomic potentials

The vast range of time and spatial scales in material computational simulations, from quantum-level calculations to macroscopic continuum models, results in a diverse array of simulation software and data formats tailored to specific applications. Therefore, standard datasets play a crucial role in the development and evaluation of MLIPs. These datasets serve as the foundational tools upon which the robustness, accuracy, and versatility of MLIPs are built and assessed. Standard datasets provide a common ground for benchmarking various MLIP models. By training and testing different MLIPs on the same dataset, researchers can objectively compare their performance, ensuring a fair and consistent evaluation of different approaches. Particularly, the diversity and comprehensiveness of high-quality standard datasets are essential for training and validating MLIPs, which determine the generalization capability of the models. In order to learn a broader spectrum of atomic interactions, the initial datasets must cover a wide range of chemical compositions, crystal structures, and physical conditions.

To overcome the lack of standardized, universal material datasets for MLIPs, firstly, the development of unified data formats and interoperability standards across different simulation software will facilitate data sharing and integration, such as Pymatgen,<sup>215</sup> ASE,<sup>216</sup> and so forth. Secondly, establishing centralized databases for material properties, accessible to researchers worldwide, could promote data standardization, consisting of material structure databases, such as Materials Project,<sup>217</sup> AFLOW,<sup>119,218</sup> Materials Cloud,<sup>120</sup> and ALKEMIE-Matter DB.<sup>122</sup> Finally, leveraging machine learning and artificial intelligence to harmonize and translate between different data formats could bridge the gap between diverse datasets, enhancing the field's overall efficiency. Recently, Justin et al.<sup>47</sup> reported the ANI-1ccx and ANI-1x datasets, which especially can be used to build generalized and accurate ML models and assess the accuracy of different models.

### Trade-off between accuracy and complexity in machine learning interatomic potentials

The development of MLIPs often faces a critical trade-off between accuracy and complexity. As the complexity of an MLIP increases to achieve higher accuracy, the computational efficiency typically decreases. This can negate one of the main advantages of MLIPs over traditional ab initio methods, which is to enable faster and larger-scale simulations. In addition, a more complex MLIP might fit the training data exceptionally well, but lead to poor performance on unseen data. Finally, complex models may not scale well with system size, limiting their applicability to larger systems or longer time scales, which are often the primary motivation for using MLIPs. Therefore, it is preferable to construct models with minimal complexity while ensuring accuracy for specific material problems.

To balance accuracy and complexity in ML models, feature engineering and dimensionality reduction methods are essential to improve the quality of datasets while retrieving material information from the data ocean. In the training process, regularization techniques such as Lasso or Ridge are utilized to prevent overfitting without overly simplifying the model. Additionally, cross-validation and ensemble methods are used to combine multiple models to improve accuracy without significantly increasing individual model complexity. Lastly, iterative refinement, by gradually adjusting model complexity based on performance metrics, can ensure a balanced approach, optimizing both accuracy and computational efficiency.

### Transferability and generalization

Training MLIPs involves datasets of immense complexity and size, whose cost associated with gathering data, computational processing, and model training is significant. Therefore, transferability and generalization are cornerstone features that determine the practical usefulness of MLIPs in diverse computational simulations. Transferable and generalizable MLIPs can accurately predict the potential energy surface for a wide range of chemical elements and compounds, not just those included in the training dataset. This is crucial for the exploration of materials and chemical phenomena. If MLIPs can generalize well, it reduces the need to create and train other models for every unique material system, saving computational resources and time.

To extend MLIP models that are applicable across various materials, incorporating a diverse dataset representing a broad range of materials and their properties can enhance the model's generalizability. Second, using transfer learning techniques allows models trained on one material to adapt to new materials with minimal additional training. Finally, developing models with scalable architectures (such as the Transformer model in large language model) ensures they can handle the complexity of different materials. In addition, a unified API for MLIPs supports the integration of these models into existing computational frameworks, enabling seamless workflow and interoperability between different simulation tools. Lastly, continuous validation and updating of the model with strange data ensure its applicability to emerging materials. This further democratizes access to advanced simulation capabilities, allowing researchers to readily apply MLIPs across various applications without needing to navigate disparate software ecosystems.

## CONCLUSIONS

In this review, the advancements and applications of MLIPs in materials science are explored, highlighting their role in overcoming the limitations of high computational costs and specificity inherent in density-functional theory and classical molecular dynamics. The four essential

stages of MLIP development are thoroughly examined, including data generation techniques, material structure descriptors, machine learning algorithms, and executable software, providing a roadmap for researchers in the field.

A significant portion of the review is dedicated to the practical applications of MLIPs in various domains such as phase-change memory materials, structural searching, material properties prediction, and the development of pre-trained universal models. These applications showcase the versatility and robustness of MLIPs in addressing complex material science challenges. Notably, the review delves into the future perspectives of MLIPs, discussing the need for standard datasets, the balance between accuracy and complexity, and the importance of transferability and generalization in these models.

In summary, this review paints a comprehensive picture of the current state and future potential of MLIPs in materials science. It underscores the transformative impact of MLIPs in bridging the gap between small-scale models and realistic device-scale simulations, thereby revolutionizing the approach to materials research and design. The advancements in MLIPs promise not only enhanced efficiency and accuracy but also open new horizons for material discovery and innovation.

## ACKNOWLEDGMENTS

This work is financially supported by the National Key Research and Development Program of China (Grant No. 2022YFB3807200), the National Natural Science Foundation of China (Grant No. 52332005), and the China Postdoctoral Science Foundation (Grant No. 2022TQ0019).

## AUTHOR CONTRIBUTIONS

Conceptualization, G. W., J. Z., and Z. S.; investigation, G. W., C. W., X. Z., and Z. L.; resources, G. W., C. W., X. Z., and Z. L.; writing – original draft, G. W., J. Z., and Z. S.; writing – review and editing, G. W., J. Z., and Z. S.; funding acquisition, G. W., J. Z., and Z. S.; supervision J. Z. and Z. S.

## DECLARATION OF INTERESTS

The authors declare no financial interest.

## REFERENCES

- Wuttig, M., and Yamada, N. (2007). Phase-change materials for rewriteable data storage. *Nat. Mater.* 6, 824–832. <https://doi.org/10.1038/nmat2009>.
- Lencer, D., Salina, M., Grabowski, B., Hikel, T., Neugebauer, J., and Wuttig, M. (2008). A map for phase-change materials. *Nat. Mater.* 7, 972–977. <https://doi.org/10.1038/nmat2330>.
- Wong, H.-S.P., and Salahuddin, S. (2015). Memory leads the way to better computing. *Nat. Nanotechnol.* 10, 191–194. <https://doi.org/10.1038/nnano.2015.29>.
- Ielmini, D., and Wong, H.-S.P. (2018). In-memory computing with resistive switching devices. *Nat. Electron.* 1, 333–343. <https://doi.org/10.1038/s41928-018-0092-2>.
- Feldmann, J., Youngblood, N., Karpov, M., Gehring, H., Li, X., Stappers, M., Le Gallo, M., Fu, X., Lukashchuk, A., Raja, A.S., et al. (2021). Parallel convolutional processing using an integrated photonic tensor core. *Nature* 589, 52–58. <https://doi.org/10.1038/s41586-020-03070-1>.
- Varnava, C. (2021). Phase-change memory devices for on-chip neural networks. *Nat. Electron.* 4, 454. <https://doi.org/10.1038/s41928-021-00627-4>.
- Jung, S., Lee, H., Myung, S., Kim, H., Yoon, S.K., Kwon, S.-W., Ju, Y., Kim, M., Yi, W., Han, S., et al. (2022). A crossbar array of magnetoresistive memory devices for in-memory computing. *Nature* 601, 211–216. <https://doi.org/10.1038/s41586-021-04196-6>.
- Maier, W.F., Stöwe, K., and Sieg, S. (2007). Combinatorial and high-throughput materials science. *Angew. Chem. Int. Ed.* 46, 6016–6067. <https://doi.org/10.1002/anie.200603675>.
- Zhao, J.-C. (2001). A combinatorial approach for structural materials. *Adv. Eng.* 14, 109673, May 17, 2024
- Wuttig, M., and Yamada, N. (2007). Phase-change materials for rewriteable data storage. *Nat. Mater.* 6, 824–832. <https://doi.org/10.1038/nmat2009>.
- Su, Y., Fu, H., Bai, Y., Jiang, X., and Xie, J. (2020). Progress in materials genome engineering in china. *Acta Metall. Sin.* 56, 1313–1323. <https://doi.org/10.11900/0412.1961.2020.00199>.
- Himanen, L., Geurts, A., Foster, A.S., and Rinke, P. (2019). Data-driven materials science: status, challenges, and perspectives. *Adv. Sci.* 6, 1900808. <https://doi.org/10.1002/advs.201900808>.
- Wang, Z., Sun, Z., Yin, H., Liu, X., Wang, J., Zhao, H., Pang, C.H., Wu, T., Li, S., Yin, Z., and Yu, X.F. (2022). Data-Driven materials innovation and applications. *Adv. Mater.* 34, 2104113. <https://doi.org/10.1002/adma.202104113>.
- Rajan, K. (2015). Materials informatics: the materials “gene” and big data. *Annu. Rev. Mater. Res.* 45, 153–169. <https://doi.org/10.1146/annurev-matsci-070214-021132>.
- Agrawal, A., and Choudhary, A. (2016). Perspective: materials informatics and big data: realization of the “fourth paradigm” of science in materials science. *Apl. Mater.* 4, 053208. <https://doi.org/10.1033/1.4946894>.
- Zhou, J., Li, P., Zhou, Y., Wang, B., Zang, J., and Meng, L. (2018). Toward new-generation intelligent manufacturing. *Engineering* 4, 11–20. <https://doi.org/10.1016/j.eng.2018.01.002>.
- Zhong, R.Y., Xu, X., Klotz, E., and Newman, S.T. (2017). Intelligent manufacturing in the context of industry 4.0: a review. *Engineering* 3, 616–630. <https://doi.org/10.1016/j.ENG.2017.05.015>.
- Behler, J. (2016). Perspective: machine learning potentials for atomistic simulations. *J. Chem. Phys.* 145, 170901. <https://doi.org/10.1063/1.4966192>.
- Watanabe, S., Li, W., Jeong, W., Lee, D., Shimizu, K., Mimanitani, E., Ando, Y., and Han, S. (2020). High-dimensional neural network atomic potentials for examining energy materials: some recent simulations. *JPhys Energy* 3, 012003. <https://doi.org/10.1088/2515-7655/abc7f3>.
- Mueller, T., Hernandez, A., and Wang, C. (2020). Machine learning for interatomic potential models. *J. Chem. Phys.* 152, 050902. <https://doi.org/10.1063/1.5126336>.
- Mishin, Y. (2021). Machine-learning interatomic potentials for materials science. *Acta Mater.* 214, 116980. <https://doi.org/10.1016/j.actamat.2021.116980>.
- Poltavsky, I., and Tkatchenko, A. (2021). Machine learning force fields: recent advances and remaining challenges. *J. Phys. Chem. Lett.* 12, 6551–6564. <https://doi.org/10.1021/acs.jpclett.1c01204>.
- Palos, E., Dasgupta, S., Lambros, E., and Paesani, F. (2023). Data-driven many-body potentials from density functional theory for aqueous phase chemistry. *Chem. Phys. Rev.* 4, 011301. <https://doi.org/10.1063/5.0129613>.
- Deringer, V.L., Bartók, A.P., Bernstein, N., Wilkins, D.M., Ceriotti, M., and Csányi, G. (2021). Gaussian process regression for materials and molecules. *Chem. Rev.* 121, 10073–10141. <https://doi.org/10.1021/acs.chemrev.1c00022>.
- Musil, F., Grisafi, A., Bartók, A.P., Ortner, C., Csányi, G., and Ceriotti, M. (2021). Physics-inspired structural representations for molecules and materials. *Chem. Rev.* 121, 9759–9815. <https://doi.org/10.1021/acs.chemrev.1c00021>.
- Westermayr, J., and Marquetand, P. (2021). Machine learning for electronically excited states of molecules. *Chem. Rev.* 121, 9759–9815. <https://doi.org/10.1021/acs.chemrev.1c00021>.

- 121, 9873–9926. <https://doi.org/10.1021/acs.chemrev.0c00749>.
26. Pinheiro, M., Ge, F., Ferré, N., Dral, P.O., and Barbatti, M. (2021). Choosing the right molecular machine learning potential. *Chem. Sci.* 12, 14396–14413. <https://doi.org/10.1039/d1sc03564a>.
27. Young, T.A., Johnston-Wood, T., Deringer, V.L., and Duarte, F. (2021). A transferable active-learning strategy for reactive molecular force fields. *Chem. Sci.* 12, 10944–10955. <https://doi.org/10.1039/d1sc01825f>.
28. Deringer, V.L., Caro, M.A., Jana, R., Arava, A., Elliott, S.R., Laurila, T., Csányi, G., and Pastewka, L. (2018). Computational surface chemistry of tetrahedral amorphous carbon by combining machine learning and density functional theory. *Chem. Mater.* 30, 7438–7445. <https://doi.org/10.1021/ACS.CHEMMATER.8B02410>.
29. Hajinazar, S., Thorn, A., Sandoval, E.D., Kharabadez, S., and Kolmogorov, A.N. (2021). MAISE: construction of neural network interatomic models and evolutionary structure optimization. *Comput. Phys. Commun.* 259, 107679. <https://doi.org/10.1016/J.CPC.2020.107679>.
30. Zhou, Y., Zhang, W., Ma, E., and Deringer, V.L. (2023). Device-scale atomistic modelling of phase-change memory materials. *Nat. Electron.* 8, 746–750. <https://doi.org/10.1038/s41928-023-01030-x>.
31. Merchant, A., Batzner, S., Schoenholz, S.S., Aykol, M., Cheon, G., and Cubuk, E.D. (2023). Scaling deep learning for materials discovery. *Nature* 624, 80–85. <https://doi.org/10.1038/s41586-023-06735-9>.
32. Unke, O.T., Chmiela, S., Gastegger, M., Schütt, K.T., Sauceda, H.E., and Müller, K.R. (2021). SpookyNet: learning force fields with electronic degrees of freedom and nonlocal effects. *Nat. Commun.* 12, 7273. <https://doi.org/10.1038/s41467-021-27504-0>.
33. Fedik, N., Zubatyuk, R., Kulichenko, M., Lubbers, N., Smith, J.S., Nebgen, B., Messerer, R., Li, Y.W., Boldyrev, A.I., Barros, K., et al. (2022). Extending machine learning beyond interatomic potentials for predicting molecular properties. *Nat. Rev. Chem.* 6, 653–672. <https://doi.org/10.1038/s41570-022-00416-3>.
34. Bernstein, N., Csányi, G., and Deringer, V.L. (2019). De novo exploration and self-guided learning of potential-energy surfaces. *npj Comput. Mater.* 5, 99. <https://doi.org/10.1038/s41524-019-0236-6>.
35. Li, W., and Ando, Y. (2018). Comparison of different machine learning models for the prediction of forces in copper and silicon dioxide. *Phys. Chem. Chem. Phys.* 20, 30006–30020. <https://doi.org/10.1039/c8cp04508a>.
36. Eckhoff, M., and Behler, J. (2021). High-dimensional neural network potentials for magnetic systems using spin-dependent atom-centered symmetry functions. *npj Comput. Mater.* 7, 170. <https://doi.org/10.1038/s41524-021-00636-z>.
37. Hernandez, A., Balasubramanian, A., Yuan, F., Mason, S.A.M., and Mueller, T. (2019). Fast, accurate, and transferable many-body interatomic potentials by symbolic regression. *npj Comput. Mater.* 5, 112. <https://doi.org/10.1038/s41524-019-0249-1>.
38. Langer, M.F., Goëßmann, A., and Rupp, M. (2022). Representations of molecules and materials for interpolation of quantum-mechanical simulations via machine learning. *npj Comput. Mater.* 8, 41. <https://doi.org/10.1038/s41524-022-00721-x>.
39. Arirth, N., Hiller, B., and Behler, J. (2013). Neural network potentials for metals and oxides – first applications to copper clusters at zinc oxide. *Phys. Status Solidi* 250, 1191–1203. <https://doi.org/10.1002/pssb.201248370>.
40. Behler, J. (2011). Neural network potential-energy surfaces in chemistry: a tool for large-scale simulations. *Phys. Chem. Chem. Phys.* 13, 17930–17955. <https://doi.org/10.1039/c1cp21668f>.
41. Arirth, N., Morawietz, T., and Behler, J. (2011). High-dimensional neural-network potentials for multicomponent systems: applications to zinc oxide. *Phys. Rev. B* 83, 153101. <https://doi.org/10.1103/PHYSREVB.83.153101>.
42. Arirth, N., and Behler, J. (2012). High-dimensional neural network potentials for metal surfaces: a prototype study for copper. *Phys. Rev. B* 85, 045439. <https://doi.org/10.1103/PHYSREVB.85.045439>.
43. Szlachta, W.J., Bartók, A.P., and Csányi, G. (2014). Accuracy and transferability of gaussian approximation potential models for tungsten. *Phys. Rev. B* 90, 104108. <https://doi.org/10.1103/PHYSREVB.90.104108>.
44. Deringer, V.L., Pickard, C.J., and Csányi, G. (2018). Data-driven learning of total and local energies in elemental boron. *Phys. Rev. Lett.* 120, 156001. <https://doi.org/10.1103/PhysRevLett.120.156001>.
45. Li, Z., Kermode, J.R., and De Vita, A. (2015). Molecular dynamics with on-the-fly machine learning of quantum-mechanical forces. *Phys. Rev. Lett.* 114, 096405. <https://doi.org/10.1103/PHYSREVLETT.114.096405>.
46. Chmiela, S., Tkatchenko, A., Sauceda, H.E., Poltavsky, I., Schütt, K.T., and Müller, K.R. (2017). Machine learning of accurate energy-conserving molecular force fields. *Sci. Adv.* 3, e1603015. <https://doi.org/10.1126/sciadv.1603015>.
47. Smith, J.S., Zubatyuk, R., Nebgen, B., Lubbers, N., Barros, K., Roitberg, A.E., Isayev, O., and Tretiak, S. (2020). The ani-1ccx and ani-1x data sets, coupled-cluster and density functional theory properties for molecules. *Sci. Data* 7, 134. <https://doi.org/10.1038/s41597-020-0473-z>.
48. Daw, M.S., Foiles, S.M., and Baskes, M.I. (1993). The embedded-atom method: a review of theory and applications. *Mater. Sci. Rep.* 9, 251–310. [https://doi.org/10.1016/0920-2307\(93\)90001-U](https://doi.org/10.1016/0920-2307(93)90001-U).
49. Finnis, M.W., and Sinclair, J.E. (1984). A simple empirical n-body potential for transition metals. *Philos. Mag. A* 50, 45–55. <https://doi.org/10.1080/01418618408244210>.
50. Tersoff, J. (1988). New empirical approach for the structure and energy of covalent systems. *Phys. Rev. B* 37, 6991–7000. <https://doi.org/10.1103/PhysRevB.37.6991>.
51. Brenner, D.W. (1990). Empirical potential for hydrocarbons for use in simulating the chemical vapor deposition of diamond films. *Phys. Rev. B* 42, 9458–9471. <https://doi.org/10.1103/PhysRevB.42.9458>.
52. Stillinger, F.H., and Weber, T.A. (1985). Computer simulation of local order in condensed phases of silicon. *Phys. Rev. B* 31, 5262–5271. <https://doi.org/10.1103/PhysRevB.31.5262>.
53. Burke, K. (2012). Perspective on density functional theory. *J. Chem. Phys.* 136, 150901. <https://doi.org/10.1063/1.4704546>.
54. Cohen, A.J., Mori-Sánchez, P., and Yang, W. (2012). Challenges for density functional theory. *Chem. Rev.* 112, 289–320. <https://doi.org/10.1021/cr200107z>.
55. Bartók, A.P., Kermode, J., Bernstein, N., and Csányi, G. (2018). Machine learning a general-purpose interatomic potential for silicon. *Phys. Rev. X* 8, 041048. <https://doi.org/10.1103/PhysRevX.8.041048>.
56. Voulodimos, A., Doulamis, N., Doulamis, A., and Protopapadakis, E. (2018). Deep learning for computer vision: a brief review. *Comput. Intell. Neurosci.* 2018, 7068349. <https://doi.org/10.1155/2018/7068349>.
57. Kamilaris, A., and Prenafeta-Boldú, F.X. (2018). Deep learning in agriculture: a survey. *Comput. Electron. Agric.* 147, 70–90. <https://doi.org/10.1016/j.compag.2018.02.016>.
58. Guo, Y., Liu, Y., Oerlemans, A., Lao, S., Wu, S., and Lew, M.S. (2016). Deep learning for visual understanding: a review. *Neurocomputing* 187, 27–48. <https://doi.org/10.1016/j.neucom.2015.09.116>.
59. LeCun, Y., Bengio, Y., and Hinton, G. (2015). Deep learning. *Nature* 521, 436–444. <https://doi.org/10.1038/nature14539>.
60. Jordan, M.I., and Mitchell, T.M. (2015). Machine learning: trends, perspectives, and prospects. *Science* 349, 255–260. <https://doi.org/10.1126/science.aaa8415>.
61. Sosso, G.C., Miceli, G., Caravati, S., Behler, J., and Bernasconi, M. (2012). Neural network interatomic potential for the phase change material GeTe. *Phys. Rev. B* 85, 174103. <https://doi.org/10.1103/PhysRevB.85.174103>.
62. Behler, J. (2011). Atom-centered symmetry functions for constructing high-dimensional neural network potentials. *J. Chem. Phys.* 134, 074106. <https://doi.org/10.1063/1.3553717>.
63. Yoo, D., Lee, K., Jeong, W., Lee, D., Watanabe, S., and Han, S. (2019). Atomic energy mapping of neural network potential. *Phys. Rev. Mater.* 3, 093802. <https://doi.org/10.1103/PhysRevMaterials.3.093802>.
64. Balyakin, I.A., Rempel, S.V., Ryltsev, R.E., and Rempel, A.A. (2020). Deep machine learning interatomic potential for liquid silica. *Phys. Rev. E* 102, 052125. <https://doi.org/10.1103/PhysRevE.102.052125>.
65. Liu, H., Fu, Z., Li, Y., Sabri, N.F.A., and Bauchy, M. (2019). Parameterization of empirical forcefields for glassy silica using machine learning. *MRS Commun.* 9, 593–599. <https://doi.org/10.1557/mrc.2019.47>.
66. Malshe, M., Narulkar, R., Raff, L.M., Hagan, M., Bukkapatnam, S., Agrawal, P.M., and Komanduri, R. (2009). Development of generalized potential-energy surfaces using many-body expansions, neural networks, and moiety energy approximations. *J. Chem. Phys.* 130, 184102. <https://doi.org/10.1063/1.3124802>.
67. Amabilino, S., Bratholm, L.A., Bennie, S.J., Vaucher, A.C., Reiher, M., and Glowacki, D.R. (2019). Training neural nets to learn reactive potential energy surfaces using interactive quantum chemistry in virtual reality. *J. Phys. Chem. A* 123, 4486–4499. <https://doi.org/10.1021/acs.jpca.9b01006>.
68. Sosso, G.C., Deringer, V.L., Elliott, S.R., and Csányi, G. (2018). Understanding the

- thermal properties of amorphous solids using machine-learning-based interatomic potentials. *Mol. Simul.* 44, 866–880. <https://doi.org/10.1080/08927022.2018.1447107>.
69. Blank, T.B., Brown, S.D., Calhoun, A.W., and Doren, D.J. (1995). Neural network models of potential energy surfaces. *J. Chem. Phys.* 103, 4129–4137. <https://doi.org/10.1063/1.469597>.
  70. Zhao, Y., Sun, J., Yang, L., Zhai, D., Sun, L., and Deng, W. (2022). Umbrella sampling with machine learning potentials applied for solid phase transition of GeSbTe. *Chem. Phys. Lett.* 803, 139813. <https://doi.org/10.1016/j.cplett.2022.139813>.
  71. Yao, K., Herr, J.E., Brown, S.N., and Parkhill, J. (2017). Intrinsic bond energies from a bonds-in-molecules neural network. *J. Phys. Chem. Lett.* 8, 2689–2694. <https://doi.org/10.1021/acs.jpcllett.7b01072>.
  72. Misawa, M., Fukushima, S., Koura, A., Shimamura, K., Shimojo, F., Tiwari, S., Nomura, K.I., Kalita, R.K., Nakano, A., and Vashishta, P. (2020). Application of first-principles-based artificial neural network potentials to multiscale-shock dynamics simulations on solid materials. *J. Phys. Chem. Lett.* 11, 4536–4541. <https://doi.org/10.1021/acs.jpcllett.0c00637>.
  73. Artrith, N., Urban, A., and Ceder, G. (2017). Efficient and accurate machine-learning interpolation of atomic energies in compositions with many species. *Phys. Rev. B* 96, 014112. <https://doi.org/10.1103/PhysRevB.96.014112>.
  74. Huang, Y., Chen, Y., Cheng, T., Wang, L.-W., and Goddard, W.A. (2018). Identification of the selective sites for electrochemical reduction of CO to  $C_{2+}$  products on copper nanoparticles by combining reactive force fields, density functional theory, and machine learning. *ACS Energy Lett.* 3, 2983–2988. <https://doi.org/10.1021/acsenergylett.8b01933>.
  75. Bartók, A.P., Payne, M.C., Kondor, R., and Csányi, G. (2010). Gaussian approximation potentials: the accuracy of quantum mechanics, without the electrons. *Phys. Rev. Lett.* 104, 136403. <https://doi.org/10.1103/PhysRevLett.104.136403>.
  76. Bartók, A.P., Kondor, R., and Csányi, G. (2013). On representing chemical environments. *Phys. Rev. B* 87, 184115. <https://doi.org/10.1103/PhysRevB.87.184115>.
  77. Deringer, V.L., and Csányi, G. (2017). Machine learning based interatomic potential for amorphous carbon. *Phys. Rev. B* 95, 094203. <https://doi.org/10.1103/PhysRevB.95.094203>.
  78. Deringer, V.L., Bernstein, N., Bartók, A.P., Cliffe, M.J., Kerber, R.N., Marbellia, L.E., Grey, C.P., Elliott, S.R., and Csányi, G. (2018). Realistic atomistic structure of amorphous silicon from machine-learning-driven molecular dynamics. *J. Phys. Chem. Lett.* 9, 2879–2885. <https://doi.org/10.1021/acs.jpcllett.8b00902>.
  79. Pattnaik, P., Raghunathan, S., Kalluri, T., Bhimalapuram, P., Jawahar, C.V., and Priyakumar, U.D. (2020). Machine learning for accurate force calculations in molecular dynamics simulations. *J. Phys. Chem. A* 124, 6954–6967. <https://doi.org/10.1021/acs.jpcsa.0c03926>.
  80. Stöhr, M., Medrano Sandonas, L., and Tkatchenko, A. (2020). Accurate many-body repulsive potentials for density-functional tight binding from deep tensor neural networks. *J. Phys. Chem. Lett.* 11, 6835–6843. <https://doi.org/10.1021/acs.jpcllett.0c01307>.
  81. Kobayashi, K., Nakamura, H., Yamaguchi, A., Itakura, M., Machida, M., and Okumura, M. (2021). Machine learning potentials for tobermorite minerals. *Comput. Mater. Sci.* 188, 110173. <https://doi.org/10.1016/j.commatsci.2020.110173>.
  82. Nitol, M.S., Dickel, D.E., and Barrett, C.D. (2021). Artificial neural network potential for pure zinc. *Comput. Mater. Sci.* 188, 110207. <https://doi.org/10.1016/j.commatsci.2020.110207>.
  83. Muhli, H., Chen, X., Bartók, A.P., Hernández-León, P., Csányi, G., Ala-Nissila, T., and Caro, M.A. (2021). Machine learning force fields based on local parametrization of dispersion interactions: application to the phase diagram of  $C_{60}$ . *Phys. Rev. B* 104, 054106. <https://doi.org/10.1103/PhysRevB.104.054106>.
  84. Miksch, A.M., Morawietz, T., Kästner, J., Urban, A., and Artrith, N. (2021). Strategies for the construction of machine-learning potentials for accurate and efficient atomic-scale simulations. *Mach. Learn. Sci. Technol.* 2, 031001. <https://doi.org/10.1088/2632-2153/abfd96>.
  85. Shi, M., Li, J., Tao, M., Zhang, X., and Liu, J. (2021). Artificial intelligence model for efficient simulation of monatomic phase change material antimony. *Mater. Sci. Semicond. Process.* 136, 106146. <https://doi.org/10.1016/j.mssp.2021.106146>.
  86. Yasuda, I., Kobayashi, Y., Endo, K., Hayakawa, Y., Fujiwara, K., Yajima, K., Arai, N., and Yasuoka, K. (2022). Prediction of transport property via machine learning molecular movements. Preprint at Arxiv. <https://doi.org/10.48550/arXiv.2203.03103>.
  87. Ouyang, Y., Yu, C., He, J., Jiang, P., Ren, W., and Chen, J. (2022). Accurate description of high-order phonon anharmonicity and lattice thermal conductivity from molecular dynamics simulations with machine learning potential. *Phys. Rev. B* 105, 115202. <https://doi.org/10.1103/PhysRevB.105.115202>.
  88. Xu, M., Xu, M., and Miao, X. (2022). Deep machine learning unravels the structural origin of mid-gap states in chalcogenide glass for high-density memory integration. *InfoMat* 4, e12315. <https://doi.org/10.1002/inf2.12315>.
  89. Li, Y.-F., and Liu, Z.-P. (2022). Smallest stable Si/SiO<sub>2</sub> interface that suppresses quantum tunneling from machine-learning-based global search. *Phys. Rev. Lett.* 128, 226102. <https://doi.org/10.1103/PhysRevLett.128.226102>.
  90. Rasheeda, D.S., Daria, A.M.S., Schröder, B., Mátyus, E., and Behler, J. (2022). High-dimensional neural network potentials for accurate vibrational frequencies: the formic acid dimer benchmark. *Phys. Chem. Chem. Phys.* 24, 29381–29392. <https://doi.org/10.1039/DCCP03893E>.
  91. Yu, W., Zhang, Z., Wan, X., Su, J., Gui, Q., Guo, H., Zhong, H.X., Robertson, J., and Guo, Y. (2023). High-accuracy machine-learned interatomic potentials for the phase change material Ge<sub>3</sub>Sb<sub>6</sub>Te<sub>5</sub>. *Chem. Mater.* 35, 6651–6658. <https://doi.org/10.1021/acs.chemmater.3c00524>.
  92. Lanzoni, D., Rovaris, F., and Montalenti, F. (2022). Machine learning potential for interacting dislocations in the presence of free surfaces. *Sci. Rep.* 12, 3760. <https://doi.org/10.1038/s41598-022-07585-7>.
  93. Wang, X.-D., Zhou, W., Zhang, H., Ahmed, S., Huang, T., Mazzarello, R., Ma, E., and Zhang, W. (2023). Multiscale simulations of growth-dominated Sb<sub>2</sub>Te phase-change material for non-volatile photonic applications. *npj Comput. Mater.* 9, 136. <https://doi.org/10.1038/s41524-023-01098-1>.
  94. Roy Chowdhury, P., Feng, T., and Ruan, X. (2019). Development of interatomic potentials for the complex binary compound Sb<sub>2</sub>Te<sub>3</sub> and the prediction of thermal conductivity. *Phys. Rev. B* 99, 155202. <https://doi.org/10.1103/PhysRevB.99.155202>.
  95. Behler, J. (2021). Four generations of high-dimensional neural network potentials. *Chem. Rev.* 121, 10037–10072. <https://doi.org/10.1021/acs.chemrev.0c00868>.
  96. Ko, T.W., Finkler, J.A., Goedecker, S., and Behler, J. (2021). General-purpose machine learning potentials capturing nonlocal charge transfer. *Acc. Chem. Res.* 54, 808–817. <https://doi.org/10.1021/acs.accounts.0c00689>.
  97. Ko, T.W., Finkler, J.A., Goedecker, S., and Behler, J. (2021). A fourth-generation high-dimensional neural network potential with accurate electrostatics including non-local charge transfer. *Nat. Commun.* 12, 398. <https://doi.org/10.1038/s41467-020-20427-2>.
  98. Deringer, V.L., Caro, M.A., and Csányi, G. (2019). Machine learning interatomic potentials as emerging tools for materials science. *Adv. Mater.* 31, 1902765. <https://doi.org/10.1002/adma.201902765>.
  99. Friederich, P., Häse, F., Proppe, J., and Aspuru-Guzik, A. (2021). Machine-learned potentials for next-generation matter simulations. *Nat. Mater.* 20, 750–761. <https://doi.org/10.1038/s41563-020-0777-6>.
  100. Unke, O.T., Chmiela, S., Sauceda, H.E., Gastegger, M., Poltavsky, I., Schütt, K.T., Tkatchenko, A., and Müller, K.R. (2021). Machine learning force fields. *Chem. Rev.* 121, 10142–10186. <https://doi.org/10.1021/acs.chemrev.0c01111>.
  101. Raccuglia, P., Elbert, K.C., Adler, P.D.F., Falk, C., Wenny, M.B., Mollo, A., Zeller, M., Friedler, S.A., Schrier, J., and Norquist, A.J. (2016). Machine-learning-assisted materials discovery using failed experiments. *Nature* 533, 73–76. <https://doi.org/10.1038/nature17439>.
  102. Raissi, M., Perdikaris, P., and Karniadakis, G.E. (2019). Physics-informed neural networks: a deep learning framework for solving forward and inverse problems involving nonlinear partial differential equations. *J. Comput. Phys.* 378, 686–707. <https://doi.org/10.1016/j.jcp.2018.10.045>.
  103. (2019). Nature Editorial Data mining uncovers a treasure trove of topological materials. *Nature* 566, 425. <https://doi.org/10.1038/d41586-019-00660-6>.
  104. Tshitoyan, V., Dagdelen, J., Weston, L., Dunn, A., Rong, Z., Kononova, O., Persson, K.A., Ceder, G., and Jain, A. (2019). Unsupervised word embeddings capture latent knowledge from materials science literature. *Nature* 571, 95–98. <https://doi.org/10.1038/s41586-019-1335-8>.
  105. Shields, B.J., Stevens, J., Li, J., Parasram, M., Damani, F., Alvarado, J.I.M., Janey, J.M., Adams, R.P., and Doyle, A.G. (2021). Bayesian reaction optimization as a tool for chemical synthesis. *Nature* 590, 89–96.

- <https://doi.org/10.1038/s41586-021-03213-y>.
106. Karniadakis, G.E., Kevrekidis, I.G., Lu, L., Perdikaris, P., Wang, S., and Yang, L. (2021). Physics-informed machine learning. *Nat. Rev. Phys.* 3, 422–440. <https://doi.org/10.1038/s42254-021-00314-5>.
107. Lu, H., Diaz, D.J., Czarnecki, N.J., Zhu, C., Kim, W., Shroff, R., Acosta, D.J., Alexander, B.R., Cole, H.O., Zhang, Y., et al. (2022). Machine learning-aided engineering of hydrolases for pet depolymerization. *Nature* 604, 662–667. <https://doi.org/10.1038/s41586-022-04599-z>.
108. Rao, Z., Tung, P.-Y., Xie, R., Wei, Y., Zhang, H., Ferrari, A., Klaver, T.P.C., Körmann, F., Sukumar, P.T., Kwiatkowski da Silva, A., et al. (2022). Machine learning–enabled high-entropy alloy discovery. *Science* 378, 78–85. <https://doi.org/10.1126/science.abo4940>.
109. Schleider, G.R., Padilha, A.C.M., Acosta, C.M., Costa, M., and Fazzio, A. (2019). From DFT to machine learning: recent approaches to materials science—a review. *J. Phys. Mater.* 2, 032001. <https://doi.org/10.1088/2515-7639/ab084b>.
110. Carleo, G., Cirac, I., Cranmer, K., Daudet, L., Schuld, M., Tishby, N., Vogt-Maranto, L., and Zdeborová, L. (2019). Machine learning and the physical sciences. *Rev. Mod. Phys.* 91, 045002. <https://doi.org/10.1103/RevModPhys.91.045002>.
111. Chen, C., Zuo, Y., Ye, W., Li, X., Deng, Z., and Ong, S.P. (2020). A critical review of machine learning of energy materials. *Adv. Energy Mater.* 10, 1903242. <https://doi.org/10.1002/aenm.201903242>.
112. Morgan, D., and Jacobs, R. (2020). Opportunities and challenges for machine learning in materials science. *Annu. Rev. Mater. Res.* 50, 71–103. <https://doi.org/10.1146/annurev-matsci-070218-010015>.
113. Chen, A., Zhang, X., and Zhou, Z. (2020). Machine learning: accelerating materials development for energy storage and conversion. *InfoMat* 2, 553–576. <https://doi.org/10.1002/inf2.12094>.
114. Gubernatis, J.E., and Lookman, T. (2018). Machine learning in materials design and discovery: examples from the present and suggestions for the future. *Phys. Rev. Mater.* 2, 120301. <https://doi.org/10.1103/PhysRevMaterials.2.120301>.
115. Batra, R., Song, L., and Ramprasad, R. (2020). Emerging materials intelligence ecosystems propelled by machine learning. *Nat. Rev. Mater.* 6, 655–678. <https://doi.org/10.1038/s41578-020-00255-y>.
116. Pilania, G. (2021). Machine learning in materials science: from explainable predictions to autonomous design. *Comput. Mater. Sci.* 193, 110360. <https://doi.org/10.1016/j.commatsci.2021.110360>.
117. Belsky, A., Hellenbrandt, M., Karen, V.L., and Luksch, P. (2002). New developments in the inorganic crystal structure database (ICSD): accessibility in support of materials research and design. *Acta Crystallogr. B* 58, 364–369. <https://doi.org/10.1107/S0108768102006948>.
118. Jain, A., Ong, S.P., Hautier, G., Chen, W., Richards, W.D., Dacek, S., Cholia, S., Gunter, D., Skinner, D., Ceder, G., and Persson, K.A. (2013). Commentary: the materials project: a materials genome approach to accelerating materials innovation. *Apl. Mater.* 1, 011002. <https://doi.org/10.1063/1.4812323>.
119. Curtarolo, S., Setyawan, W., Hart, G.L., Jahnatek, M., Chepulskii, R.V., Taylor, R.H., Wang, S., Xue, J., Yang, K., Levy, O., et al. (2012). AFLOW: an automatic framework for high-throughput materials discovery. *Comput. Mater. Sci.* 58, 218–226. <https://doi.org/10.1016/j.commatsci.2012.02.005>.
120. Pizzi, G., Cepellotti, A., Sabatini, R., Marzari, N., and Kozinsky, B. (2016). AllIDA: automated interactive infrastructure and database for computational science. *Comput. Mater. Sci.* 111, 218–230. <https://doi.org/10.1016/j.commatsci.2015.09.013>.
121. Draxl, C., and Scheffler, M. (2019). The nomad laboratory: from data sharing to artificial intelligence. *J. Phys. Mater.* 2, 036001. <https://doi.org/10.1088/2515-7639/ab13bb>.
122. Wang, G., Peng, L., Li, K., Zhu, L., Zhou, J., Miao, N., and Sun, Z. (2021). ALKEMIE: an intelligent computational platform for accelerating materials discovery and design. *Comput. Mater. Sci.* 186, 110064. <https://doi.org/10.1016/j.commatsci.2020.110064>.
123. Wang, G., Li, K., Peng, L., Zhang, Y., Zhou, J., and Sun, Z. (2021). High-throughput automatic integrated material calculations and data management intelligent platform and the application in novel alloys. *Acta Metall. Sin.* 48, 75–87. <https://doi.org/10.11900/0412.1961.2021.00041>.
124. Sun, Y., Wang, G., Li, K., Peng, L., Zhou, J., and Sun, Z. (2023). Accelerating the discovery of transition metal borides by machine learning on small data sets. *ACS Appl. Mater. Interfaces* 15, 29278–29286. <https://doi.org/10.1021/acsami.3c03657>.
125. Saal, J.E., Kirklin, S., Aykol, M., Meredig, B., and Wolverton, C. (2013). Materials design and discovery with high-throughput density functional theory: the open quantum materials database (OQMD). *JOM* 65, 1501–1509. <https://doi.org/10.1007/s11837-013-0755-4>.
126. Quirós, M., Gražulis, S., Girdzijauskaitė, S., Merkys, A., and Vaikus, A. (2018). Using smiles strings for the description of chemical connectivity in the crystallography open database. *J. Cheminf.* 10, 23. <https://doi.org/10.1186/s13321-018-0279-6>.
127. Borysov, S.S., Geilhufe, R.M., and Balatsky, A.V. (2017). Organic materials database: an open-access online database for data mining. *PLoS One* 12, e0171501. <https://doi.org/10.1371/journal.pone.0171501>.
128. Haastrup, S., Strange, M., Pandey, M., Deilmann, T., Schmidt, P.S., Hinsche, N.F., Gjerdings, M.N., Torelli, D., Larsen, P.M., Riis-Jensen, A.C., et al. (2018). The computational 2D materials database: high-throughput modeling and discovery of atomically thin crystals. *2D Mater.* 5, 042002. <https://doi.org/10.1088/2053-1583/aaacf1>.
129. Tanifuji, M., Matsuda, A., and Yoshikawa, H. (2019). Materials data platform – a fair system for data-driven materials science. In 2019 8th International Congress on Advanced Applied Informatics (IIAI-AAI), pp. 1021–1022. <https://doi.org/10.1109/IIAI-AAI.2019.900206>.
130. Kalinin, S.V., Sumpter, B.G., and Archibald, R.K. (2015). Big–deep–smart data in imaging for guiding materials design. *Nat. Mater.* 14, 973–980. <https://doi.org/10.1038/nmat4395>.
131. Mehr, S.H.M., Craven, M., Leonov, A.I., Keenan, G., and Cronin, L. (2020). A universal system for digitization and automatic execution of the chemical synthesis literature. *Science* 370, 101–108. <https://doi.org/10.1126/science.abc2986>.
132. Vergniory, M.G., Wieder, B.J., Elcoro, L., Parkin, S.S.P., Felser, C., Bernevig, B.A., and Regnault, N. (2022). All topological bands of all nonmagnetic stoichiometric materials. *Science* 376, eabg9094. <https://doi.org/10.1126/science.abg9094>.
133. Zhu, L., Zhou, J., and Sun, Z. (2022). Materials data toward machine learning: advances and challenges. *J. Phys. Chem. Lett.* 13, 3965–3977.
134. Vandermause, J., Torrisi, S.B., Batzner, S., Xie, Y., Sun, L., Kolpak, A.M., and Kozinsky, B. (2020). On-the-fly active learning of interpretable bayesian force fields for atomistic rare events. *npj Comput. Mater.* 6, 20. <https://doi.org/10.1038/s41524-020-0283-z>.
135. Xue, D., Balachandran, P.V., Hogden, J., Theiler, J., Xue, D., and Lookman, T. (2016). Accelerated search for materials with targeted properties by adaptive design. *Nat. Commun.* 7, 11241. <https://doi.org/10.1038/ncomms11241>.
136. Narayanan, H., Cruz Bournazou, M.N., Guillén Gosálbez, G., and Butté, A. (2022). Functional-hybrid modeling through automated adaptive symbolic regression for interpretable mathematical expressions. *Chem. Eng. J.* 430, 133032. <https://doi.org/10.1016/j.cej.2021.133032>.
137. Behler, J., Martonák, R., Donadio, D., and Parrinello, M. (2008). Metadynamics simulations of the high-pressure phases of silicon employing a high-dimensional neural network potential. *Phys. Rev. Lett.* 100, 185501. <https://doi.org/10.1103/PHYSREVLETT.100.185501>.
138. Yang, M., Bonati, L., Polino, D., and Parrinello, M. (2022). Using metadynamics to build neural network potentials for reactive events: the case of urea decomposition in water. *Catal. Today* 387, 143–149. <https://doi.org/10.1016/j.cattod.2021.03.018>.
139. Tong, Q., Luo, X., Adeleke, A.A., Gao, P., Xie, Y., Liu, H., Li, Q., Wang, Y., Lv, J., Yao, Y., and Ma, Y. (2021). Machine learning metadynamics simulation of reconstructive phase transition. *Phys. Rev. B* 103, 054107. <https://doi.org/10.1103/PhysRevB.103.054107>.
140. Gopalakrishnan, K. (2018). Deep learning in data-driven pavement image analysis and automated distress detection: a review. *Data* 3, 28.
141. Chan, C.H., Sun, M., and Huang, B. (2022). Application of machine learning for advanced material prediction and design. *EcoMat* 4, e12194. <https://doi.org/10.1002/eom2.12194>.
142. Fu, Z., Liu, W., Huang, C., and Mei, T. (2022). A review of performance prediction based on machine learning in materials science. *Nanomaterials* 12, 2957. <https://doi.org/10.3390/nano12172957>.
143. Rodrigues, J.F., Florea, L., de Oliveira, M.C.F., Diamond, D., and Oliveira, O.N. (2021). Big data and machine learning for materials science. *Discov. Mater.* 1, 12. <https://doi.org/10.1007/s43939-021-00012-0>.
144. Zhou, T., Song, Z., and Sundmacher, K. (2019). Big data creates new opportunities for materials research: a review on methods and applications of machine learning for materials design. *Engineering* 5, 1017–1026. <https://doi.org/10.1016/j.eng.2019.02.011>.
145. White, A.A. (2013). Big data are shaping the future of materials science. *MRS Bull.* 38,

- 594–595. <https://doi.org/10.1557/mrs.2013.187>.
146. Blaiszik, B., Ward, L., Schwarting, M., Gaff, J., Chard, R., Pike, D., Chard, K., and Foster, I. (2019). A data ecosystem to support machine learning in materials science. *MRS Commun.* 9, 1125–1133.
147. Fan, W., and Bifet, A. (2013). Mining big data: current status, and forecast to the future. *SIGKDD Explor. Newsl.* 14, 1–5.
148. Kalidindi, S.R., and De Graef, M. (2015). Materials data science: current status and future outlook. *Annu. Rev. Mater. Res.* 45, 171–193. <https://doi.org/10.1146/annurev-matsci-070214-020844>.
149. Seshadri, R., and Sparks, T.D. (2016). Perspective: interactive material property databases through aggregation of literature data. *Apl. Mater.* 4, 053206. <https://doi.org/10.1063/1.4944682>.
150. Gastegger, M., Schwiedrzik, L., Bittermann, M., Berzenyi, F., and Marquetand, P. (2018). WACSF—weighted atom-centered symmetry functions as descriptors in machine learning potentials. *J. Chem. Phys.* 148, 241709. <https://doi.org/10.1063/1.5019667>.
151. Thompson, A.P., Swiler, L.P., Trott, C.R., Foiles, S.M., and Tucker, G.J. (2015). Spectral neighbor analysis method for automated generation of quantum-accurate interatomic potentials. *J. Comput. Phys.* 285, 316–330. <https://doi.org/10.1016/j.jcp.2014.12.018>.
152. Rupp, M., Tkatchenko, A., Müller, K.R., and von Lilienfeld, O.A. (2012). Fast and accurate modeling of molecular atomization energies with machine learning. *Phys. Rev. Lett.* 108, 058301. <https://doi.org/10.1103/PhysRevLett.108.058301>.
153. Faber, F., Lindmaa, A., von Lilienfeld, O.A., and Armiento, R. (2015). Crystal structure representations for machine learning models of formation energies. *Int. J. Quantum Chem.* 115, 1094–1101. <https://doi.org/10.1002/qua.24917>.
154. Huo, H., and Rupp, M. (2022). Unified representation of molecules and crystals for machine learning. *Mach. Learn. Sci. Technol.* 3, 045017. <https://doi.org/10.1088/2632-2153/aca005>.
155. Himanen, L., Jäger, M.O., Morooka, E.V., Federici Canova, F., Ranawat, Y.S., Gao, D.Z., Rinke, P., and Foster, A.S. (2020). DSScribe: library of descriptors for machine learning in materials science. *Comput. Phys. Commun.* 247, 106949. <https://doi.org/10.1016/j.cpc.2019.106949>.
156. Drautz, R. (2019). Atomic cluster expansion for accurate and transferable interatomic potentials. *Phys. Rev. B* 99, 014104. <https://doi.org/10.1103/PhysRevB.99.014104>.
157. Jain, A., and Bligaard, T. (2018). Atomic-position independent descriptor for machine learning of material properties. *Phys. Rev. B* 98, 214112. <https://doi.org/10.48550/arXiv.1809.03960>.
158. Zhang, L., Han, J., Wang, H., Car, R., and E, W. (2018). Deep potential molecular dynamics: a scalable model with the accuracy of quantum mechanics. *Phys. Rev. Lett.* 120, 143001. <https://doi.org/10.1103/PhysRevLett.120.143001>.
159. Xie, T., and Grossman, J.C. (2018). Crystal graph convolutional neural networks for an accurate and interpretable prediction of material properties. *Phys. Rev. Lett.* 120, 145301. <https://doi.org/10.1103/PhysRevLett.120.145301>.
160. Behler, J., and Parrinello, M. (2007). Generalized neural-network representation of high-dimensional potential-energy surfaces. *Phys. Rev. Lett.* 98, 146401. <https://doi.org/10.1103/PhysRevLett.98.146401>.
161. Kocer, E., Ko, T.W., and Behler, J. (2022). Neural network potentials: a concise overview of methods. *Annu. Rev. Phys. Chem.* 73, 163–186. <https://doi.org/10.1146/annurev-physchem-082720-034254>.
162. Smith, J.S., Isayev, O., and Roitberg, A.E. (2017). ANI-1: an extensible neural network potential with DFT accuracy at force field computational cost. *Chem. Sci.* 8, 3192–3203. <https://doi.org/10.1039/c6sc05720a>.
163. Nebgen, B., Lubbers, N., Smith, J.S., Sifain, A.E., Lokhov, A., Isayev, O., Roitberg, A.E., Barros, K., and Tretiak, S. (2018). Transferable dynamic molecular charge assignment using deep neural networks. *J. Chem. Theory Comput.* 14, 4687–4698. <https://doi.org/10.1021/acs.jctc.8b00524>.
164. López-Zorrilla, J., Aretxabaleta, X.M., Yeu, I.W., Etxebarria, I., Manzano, H., and Artrith, N. (2023). Ænet-PyTorch: a GPU-supported implementation for machine learning atomic potentials training. *J. Chem. Phys.* 158, 164105. <https://doi.org/10.1063/5.0146803>.
165. Chen, C., Ye, W., Zuo, Y., Zheng, C., and Ong, S.P. (2019). Graph networks as a universal machine learning framework for molecules and crystals. *Chem. Mater.* 31, 3564–3572. <https://doi.org/10.1021/acs.chemmater.9b01294>.
166. Chen, C., Zuo, Y., Ye, W., Li, X., and Ong, S.P. (2021). Learning properties of ordered and disordered materials from multi-fidelity data. *Nat. Comput. Sci.* 1, 46–53. <https://doi.org/10.1038/s43588-020-00002-x>.
167. Chen, B., Huang, K., Raghupathi, S., Chandratreya, I., Du, Q., and Lipson, H. (2022). Automated discovery of fundamental variables hidden in experimental data. *Nat. Comput. Sci.* 2, 433–442. <https://doi.org/10.1038/s43588-022-00281-6>.
168. Reiser, P., Neubert, M., Eberhard, A., Torresi, L., Zhou, C., Shao, C., Metni, H., Van Hoesel, C., Schopmans, H., Sommer, T., and Friedrich, P. (2022). Graph neural networks for materials science and chemistry. *Commun. Mater.* 3, 93. <https://doi.org/10.1038/s43246-022-00315-6>.
169. Yao, K., Herr, J.E., Toth, D.W., Mckintyre, R., and Parkhill, J. (2018). The TensorMol-0.1 model chemistry: a neural network augmented with long-range physics. *Chem. Sci.* 9, 2261–2269. <https://doi.org/10.1039/C7SC04934J>.
170. Gasteiger, J., Giri, S., Margraf, J.T., and Günemann, S. (2022). Fast and uncertainty-aware directional message passing for non-equilibrium molecules. Preprint at ArXiv. <https://doi.org/10.48550/arXiv.2011.14115>.
171. Gasteiger, J., Groß, J., and Günemann, S. (2022). Directional message passing for molecular graphs. Preprint at ArXiv. <https://doi.org/10.48550/arXiv.2003.03123>.
172. Batatia, I., Kovacs, D.P., Simm, G.N.C., Ortner, C., and Csányi, G. (2022). MACE: higher order equivariant message passing neural networks for fast and accurate force fields. *Adv. Neural Inf. Process. Syst.* 35, 11423–11436. <https://doi.org/10.48550/arXiv.2206.07697>.
173. Satorras, V.G., Hoogeboom, E., and Welling, M. (2022). E(n) equivariant graph neural networks. *Int. Conf. Mach. Learn.* 139, 9323–9332. <https://doi.org/10.48550/arXiv.2102.09844>.
174. Batzner, S., Musaelian, A., Sun, L., Geiger, M., Mailoa, J.P., Kornbluth, M., Molinari, N., Smidt, T.E., and Kozinsky, B. (2022). E(3)-equivariant graph neural networks for data-efficient and accurate interatomic potentials. *Nat. Commun.* 13, 2453. <https://doi.org/10.1038/s41467-022-29939-5>.
175. Qiao, Z., Christensen, A.S., Welborn, M., Manby, F.R., Anandkumar, A., and Miller, T.F., 3rd (2022). Informing geometric deep learning with electronic interactions to accelerate quantum chemistry. *Proc. Natl. Acad. Sci.* 119, e2205221119. <https://doi.org/10.1073/pnas.2205221119>.
176. Thomas, N., Smidt, T., Kearnes, S., Yang, L., Li, L., Kohlhoff, K., and Riley, P. (2018). Tensor field networks: rotation- and translation-equivariant neural networks for 3d point clouds. Preprint at ArXiv. <https://doi.org/10.48550/arXiv.1802.08219>.
177. Shapeev, A.V. (2016). Moment tensor potentials: a class of systematically improvable interatomic potentials. *Multiscale Model. Simul.* 14, 1153–1173. <https://doi.org/10.1137/15M1054183>.
178. Christensen, A.S., Bratholm, L.A., Faber, F.A., and Anatole von Lilienfeld, O. (2020). FCHL revisited: faster and more accurate quantum machine learning. *J. Chem. Phys.* 152, 044107. <https://doi.org/10.1063/1.5126701>.
179. Zaverkin, V., and Kästner, J. (2020). Gaussian moments as physically inspired molecular descriptors for accurate and scalable machine learning potentials. *J. Chem. Theory Comput.* 16, 5410–5421. <https://doi.org/10.1021/acs.jctc.0c00347>.
180. Thölke, P., and De Fabritiis, G. (2022). TorchMD-net: equivariant transformers for neural network based molecular potentials. Preprint at ArXiv. <https://doi.org/10.48550/arXiv.2202.02541>.
181. Shi, M., Mo, P., and Liu, J. (2020). Deep neural network for accurate and efficient atomistic modeling of phase change memory. *IEEE Electron. Device Lett.* 41, 365–368. <https://doi.org/10.1109/LED.2020.2964779>.
182. Sosso, G.C., and Bernasconi, M. (2019). Harnessing machine learning potentials to understand the functional properties of phase-change materials. *MRS Bull.* 44, 705–709. <https://doi.org/10.1557/mrs.2019.202>.
183. Chan, H., Narayanan, B., Cherukara, M.J., Sen, F.G., Sasikumar, K., Gray, S.K., Chan, M.K.Y., and Sankaranarayanan, S.K.R.S. (2019). Machine learning classical interatomic potentials for molecular dynamics from first-principles training data. *J. Phys. Chem. C* 123, 6941–6957. <https://doi.org/10.1021/acs.jpcc.8b09917>.
184. Mocanu, F.C., Konstantinou, K., Lee, T.H., Bernstein, N., Deringer, V.L., Csányi, G., and Elliott, S.R. (2018). Modeling the phase-change memory material,  $\text{Ge}_2\text{Sb}_2\text{Te}_5$ , with a machine-learned interatomic potential. *J. Phys. Chem. B* 122, 8998–9006. <https://doi.org/10.1021/acs.jpcb.8b06476>.
185. Ahmed, S., Wang, X., Li, H., Zhou, Y., Chen, Y., Sun, L., Zhang, W., and Mazzarello, R. (2021). Change in structure of amorphous Sb–Te phase-change materials as a function of stoichiometry. *Phys. Status Solidi Rapid Res. Lett.* 15, 2100064. <https://doi.org/10.1002/pssr.202100064>.

186. Mocanu, F.C., Konstantinou, K., and Mavra, J. (2021). On the chemical bonding of amorphous Sb<sub>2</sub>Te<sub>3</sub>. *Phys. Status Solidi Rapid Res. Lett.* 15, 2000485. <https://doi.org/10.1002/pssr.202000485>.
187. Wang, G., Sun, Y., Zhou, J., and Sun, Z. (2023). PotentialMind: graph convolutional machine learning potential for Sb–Te binary compounds of multiple stoichiometries. *J. Phys. Chem. C* 127, 24724–24733. <https://doi.org/10.1021/acs.jpcc.3c07110>.
188. Rowe, P., Csányi, G., Alfe, D., and Michaelides, A. (2018). Development of a machine learning potential for graphene. *Phys. Rev. B* 97, 054303. <https://doi.org/10.1103/PhysRevB.97.054303>.
189. Nguyen, M.-T., Rousseau, R., Paviet, P.D., and Glezakou, V.-A. (2021). Actinide molten salts: a machine-learning potential molecular dynamics study. *ACS Appl. Mater. Interfaces* 13, 53398–53408. <https://doi.org/10.1021/acsmami.1c11358>.
190. Deng, Y., Fu, S., Guo, J., Xu, X., and Li, H. (2023). Anisotropic collective variables with machine learning potential for Ab initio crystallization of complex ceramics. *ACS Nano* 17, 14099–14113. <https://doi.org/10.1021/acsnano.3c04602>.
191. Miwa, K., and Asahi, R. (2021). Molecular dynamics simulations of lithium superionic conductor Li<sub>10</sub>GeP<sub>5</sub>S<sub>12</sub> using a machine learning potential. *Solid State Ion.* 361, 115567. <https://doi.org/10.1016/j.ssi.2021.115567>.
192. Jia, W., Wang, H., Chen, M., Lu, D., Lin, L., Car, R., Weinan, E., and Zhang, L. (2020). Pushing the limit of molecular dynamics with ab initio accuracy to 100 million atoms with machine learning. In SC20: International conference for high performance computing, networking, storage and analysis, pp. 1–14. <https://doi.org/10.1109/SC41405.2020.00009>.
193. Gubaev, K., Podryabinkin, E.V., Hart, G.L., and Shapeev, A.V. (2019). Accelerating high-throughput searches for new alloys with active learning of interatomic potentials. *Comput. Mater. Sci.* 156, 148–156. <https://doi.org/10.1016/j.commatsci.2018.09.031>.
194. Mortazavi, B., Novikov, I.S., Podryabinkin, E.V., Roche, S., Rabczuk, T., Shapeev, A.V., and Zhuang, X. (2020). Exploring phononic properties of two-dimensional materials using machine learning interatomic potentials. *Appl. Mater. Today* 20, 100685. <https://doi.org/10.1016/j.apmt.2020.100685>.
195. Deringer, V.L. (2020). Modelling and understanding battery materials with machine-learning-driven atomistic simulations. *J. Phys. Energy* 2, 041003. <https://doi.org/10.1088/2515-7655/abb011>.
196. Barrett, D.H., and Haruna, A. (2020). Artificial intelligence and machine learning for targeted energy storage solutions. *Curr. Opin. Electrochem.* 21, 160–166. <https://doi.org/10.1016/j.coelec.2020.02.002>.
197. Thiemann, F.L., Rowe, P., Müller, E.A., and Michaelides, A. (2020). Machine learning potential for hexagonal boron nitride applied to thermally and mechanically induced rippling. *J. Phys. Chem. C* 124, 22278–22290. <https://doi.org/10.1021/acs.jpcc.0c05831>.
198. Seko, A. (2020). Machine learning potentials for multicomponent systems: the Ti-Al binary system. *Phys. Rev. B* 102, 174104. <https://doi.org/10.1103/PhysRevB.102.174104>.
199. Marchand, D., Jain, A., Glensk, A., and Curtin, W.A. (2020). Machine learning for metallurgy I. a neural-network potential for Al-Cu. *Phys. Rev. Mater.* 4, 103601. <https://doi.org/10.1103/PhysRevMaterials.4.103601>.
200. Arabha, S., and Rajabpour, A. (2021). Thermo-mechanical properties of nitrogenated holey graphene (C<sub>2</sub>N): a comparison of machine-learning-based and classical interatomic potentials. *Int. J. Heat Mass Transf.* 178, 121589. <https://doi.org/10.1016/j.ijheatmasstransfer.2021.121589>.
201. Fan, Z., Song, K., Zhao, R., Liu, J., Wang, Y., Lindgren, E., Wang, Y., Chen, S., Xu, K., Liang, T., et al. (2023). General-purpose machine-learned potential for 16 elemental metals and their alloys. Preprint at ArXiv. <https://doi.org/10.21203/rs.3.rs-3612294/v1>.
202. Ladygin, V.V., Korotaev, P.Y., Yanilkin, A.V., and Shapeev, A.V. (2020). Lattice dynamics simulation using machine learning interatomic potentials. *Comput. Mater. Sci.* 172, 109333. <https://doi.org/10.1016/j.commatsci.2019.109333>.
203. Liu, Y.-B., Yang, J.-Y., Xin, G.-M., Liu, L.-H., Csányi, G., and Cao, B.-Y. (2020). Machine learning interatomic potential developed for molecular simulations on thermal properties of β-Ga<sub>2</sub>O<sub>3</sub>. *J. Chem. Phys.* 153, 144501. <https://doi.org/10.1063/5.0027643>.
204. Wu, C.-W., Ren, X., Li, S.-Y., Zeng, Y.-J., Zhou, W.-X., and Xie, G. (2022). Significant regulation of stress on the contribution of optical phonons to thermal conductivity in layered Li<sub>2</sub>ZrCl<sub>6</sub>: first-principles calculations combined with the machine-learning potential approach. *Appl. Phys. Lett.* 121, 172201. <https://doi.org/10.1063/5.0122357>.
205. Zhang, G., Dong, S., Yang, C., Han, D., Xin, G., and Wang, X. (2023). Revisiting four-phonon scattering in WS<sub>2</sub> monolayer with machine learning potential. *Appl. Phys. Lett.* 123, 052205. <https://doi.org/10.1063/5.0159517>.
206. Wen, T., Wang, C.-Z., Kramer, M.J., Sun, Y., Ye, B., Wang, H., Liu, X., Zhang, C., Zhang, F., Ho, K.-M., and Wang, N. (2019). Development of a deep machine learning interatomic potential for metalloid-containing Pd-Si compounds. *Phys. Rev. B* 100, 174101. <https://doi.org/10.1103/PhysRevB.100.174101>.
207. Podryabinkin, E.V., Tikhonov, E.V., Shapeev, A.V., and Oganov, A.R. (2019). Accelerating crystal structure prediction by machine-learning interatomic potentials with active learning. *Phys. Rev. B* 99, 064114. <https://doi.org/10.1103/PhysRevB.99.064114>.
208. Nishiyama, T., Seko, A., and Tanaka, I. (2020). Application of machine learning potentials to predict grain boundary properties in fcc elemental metals. *Phys. Rev. Mater.* 4, 123607. <https://doi.org/10.1103/PhysRevMaterials.4.123607>.
209. Yokoi, T., Adachi, K., Iwase, S., and Matsunaga, K. (2022). Accurate prediction of grain boundary structures and energetics in CdTe: a machine-learning potential approach. *Phys. Chem. Chem. Phys.* 24, 1620–1629. <https://doi.org/10.1039/D1CP04329C>.
210. Takamoto, S., Shinagawa, C., Motoki, D., Nakago, K., Li, W., Kurata, I., Watanabe, T., Yayama, Y., Iriguchi, H., Asano, Y., et al. (2022). Towards universal neural network potential for material discovery applicable to arbitrary combination of 45 elements. *Nat. Commun.* 13, 2991. <https://doi.org/10.1038/s41467-022-30687-9>.
211. Chen, C., and Ong, S.P. (2022). A universal graph deep learning interatomic potential for the periodic table. *Nat. Comput. Sci.* 2, 718–728. <https://doi.org/10.1038/s43588-022-00349-3>.
212. Owen, C.J., Torrisi, S.B., Xie, Y., Batzner, S., Bystrom, K., Coulter, J., Musaelian, A., Sun, L., and Kozinsky, B. (2023). Complexity of many-body interactions in transition metals via machine-learned force fields from the TM23 data set. Preprint at ArXiv. <https://doi.org/10.48550/arXiv.2302.12993>.
213. Batatia, I., Benner, P., Chiang, Y., Elena, A.M., Kovács, D.P., Riebesell, J., Advincula, X.R., Asta, M., Baldwin, W.J., Bernstein, N., et al. (2023). A foundation model for atomistic materials chemistry. Preprint at ArXiv. <https://doi.org/10.48550/arXiv.2401.00096>.
214. Deng, B., Zhong, P., Jun, K., Riebesell, J., Han, K., Bartel, C.J., and Ceder, G. (2023). CHGNet as a pretrained universal neural network potential for charge-informed atomistic modelling. *Nat. Mach. Intell.* 5, 1031–1041. <https://doi.org/10.1038/s42256-023-00716-3>.
215. Ong, S.P., Richards, W.D., Jain, A., Hautier, G., Kocher, M., Cholia, S., Gunter, D., Chevrier, V.L., Persson, K.A., and Ceder, G. (2013). Python materials genomics ( pymatgen): a robust, open-source python library for materials analysis. *Comput. Mater. Sci.* 68, 314–319. <https://doi.org/10.1016/j.commatsci.2012.10.028>.
216. Hjorth Larsen, A., Jørgen Mortensen, J., Blomqvist, J., Castelli, I.E., Christensen, R., Dulák, M., Friis, J., Groves, M.N., Hammer, B., Hargus, C., et al. (2017). The atomic simulation environment—a python library for working with atoms. *J. Phys. Condens. Matter* 29, 273002. <https://doi.org/10.1088/1361-648x/aa680e>.
217. Jain, A., Persson, K.A., and Ceder, G. (2016). Research update: the materials genome initiative: data sharing and the impact of collaborative ab initio databases. *Apl. Mater.* 4, 053102. <https://doi.org/10.1063/1.4944683>.
218. Curtarolo, S., Setyawan, W., Wang, S., Xue, J., Yang, K., Taylor, R.H., Nelson, L.J., Hart, G.L., Sanvito, S., Buongiorno-Nardelli, M., et al. (2012). AFLOWLIB.org: a distributed materials properties repository from high-throughput ab initio calculations. *Comput. Mater. Sci.* 58, 227–235. <https://doi.org/10.1016/j.commatsci.2012.02.002>.
219. Wang, G., and Sun, Z. (2023). Atomic insights into device-scale phase-change memory materials using machine learning potential. *Sci. Bull.* 68, 3105–3107. <https://doi.org/10.1016/j.scib.2023.11.038>.
220. Imbalzano, G., Anelli, A., Giofré, D., Klees, S., Behler, J., and Ceriotti, M. (2018). Automatic selection of atomic fingerprints and reference configurations for machine-learning potentials. *J. Chem. Phys.* 148, 241730. <https://doi.org/10.1063/1.5024611>.
221. Caro, M.A. (2019). Optimizing many-body atomic descriptors for enhanced computational performance of machine learning based interatomic potentials. *Phys. Rev. B* 100, 024112. <https://doi.org/10.1103/PhysRevB.100.024112>.
222. Arirth, N., and Urban, A. (2016). An implementation of artificial neural-network potentials for atomistic materials simulations: performance for TiO<sub>2</sub>. *Comput.*

- Mater. Sci. 114, 135–150. <https://doi.org/10.1016/j.commatsci.2015.11.047>.
223. Schütt, K.T., Arbabzadah, F., Chmiela, S., Müller, K.R., and Tkatchenko, A. (2017). Quantum-chemical insights from deep tensor neural networks. Nat. Commun. 8, 13890. <https://doi.org/10.1038/ncomms13890>.
224. Schütt, K., Kindermans, P.-J., Felix, H.E.S., Chmiela, S., Tkatchenko, A., and Müller, K.-R. (2017). SchNet: a continuous-filter convolutional neural network for modeling quantum interactions. Adv. Neural Inf. Process. Syst. 30, 1–11. <https://doi.org/10.5555/3294771.3294866>.
225. Wang, H., Zhang, L., Han, J., and Weinan, E. (2018). DeePMD-kit: a deep learning package for many-body potential energy representation and molecular dynamics. Comput. Phys. Commun. 228, 178–184. <https://doi.org/10.1016/j.cpc.2018.03.016>.
226. Lu, D., Jiang, W., Chen, Y., Zhang, L., Jia, W., Wang, H., and Chen, M. (2021). DP train, then dp compress: model compression in deep potential molecular dynamics. Preprint at ArXiv. <https://doi.org/10.48550/arXiv.2107.02103>.
227. Unke, O.T., and Meuwly, M. (2019). PhysNet: a neural network for predicting energies, forces, dipole moments, and partial charges. J. Chem. Theory Comput. 15, 3678–3693. <https://doi.org/10.1021/acs.jctc.9b00181>.
228. Finzi, M., Stanton, S., Izmailov, P., and Wilson, A.G. (2020). Generalizing convolutional neural networks for equivariance to lie groups on arbitrary continuous data. Int. Conf. Mach. Learn. 119, 3165–3176. <https://doi.org/10.48550/arXiv.2002.12880>.
229. Fan, Z., Zeng, Z., Zhang, C., Wang, Y., Song, K., Dong, H., Chen, Y., and Ala-Nissila, T. (2021). Neuroevolution machine learning potentials: combining high accuracy and low cost in atomistic simulations and application to heat transport. Phys. Rev. B 104, 104309. <https://doi.org/10.1103/PhysRevB.104.104309>.
230. Park, C.W., Kornbluth, M., Vandermause, J., Wolverton, C., Kozinsky, B., and Mailoa, J.P. (2021). Accurate and scalable graph neural network force field and molecular dynamics with direct force architecture. npj Comput. Mater. 7, 73. <https://doi.org/10.1038/s41524-021-00543-3>.
231. Wang, Z., Wang, C., Zhao, S., Du, S., Xu, Y., Gu, B.-L., and Duan, W. (2021). Symmetry-adapted graph neural networks for constructing molecular dynamics force fields. Sci. China Phys. Mech. Astron. 64, 117211. <https://doi.org/10.1007/s11433-021-1739-4>.
232. Godwin, J., Schaarschmidt, M., Gaunt, A., Sanchez-Gonzalez, A., Rubanova, Y., Velicković, P., Kirkpatrick, J., and Battaglia, P. (2022). Simple gnn regularisation for 3d molecular property prediction & beyond. Preprint at ArXiv. <https://doi.org/10.48550/arXiv.2106.07971>.
233. Takamoto, S., Izumi, S., and Li, J. (2022). TeaNet: universal neural network interatomic potential inspired by iterative electronic relaxations. Comput. Mater. Sci. 207, 111280. <https://doi.org/10.1016/j.commatsci.2022.111280>.
234. Haghhighatlari, M., Li, J., Guan, X., Zhang, O., Das, A., Stein, C.J., Heidar-Zadeh, F., Liu, M., Head-Gordon, M., Bertels, L., et al. (2022). NewtonNet: a newtonian message passing network for deep learning of interatomic potentials and forces. Digit. Discov. 1, 333–343. <https://doi.org/10.1039/D2DD00008C>.
235. Liu, Y., Wang, L., Liu, M., Zhang, X., Oztekin, B., and Ji, S. (2022). Spherical message passing for 3d graph networks. Preprint at ArXiv. <https://doi.org/10.48550/arXiv.2102.05013>.
236. Schütt, K.T., Unke, O.T., and Gastegger, M. (2021). Equivariant message passing for the prediction of tensorial properties and molecular spectra. Preprint at ArXiv. <https://doi.org/10.48550/arXiv.2102.03150>.
237. Gasteiger, J., Becker, F., and Günnemann, S. (2022). Gemnet: universal directional graph neural networks for molecules. Adv. Neural Inf. Process. Syst. 34, 6790–6802. <https://doi.org/10.48550/arXiv.2106.08903>.
238. Wang, Z., Wang, C., Zhao, S., Xu, Y., Hao, S., Hsieh, C.Y., Gu, B.-L., and Duan, W. (2022). Heterogeneous relational message passing networks for molecular dynamics simulations. npj Comput. Mater. 8, 53. <https://doi.org/10.1038/s41524-022-00739-1>.
239. Musaelian, A., Batzner, S., Johansson, A., Sun, L., Owen, C.J., Kornbluth, M., and Kozinsky, B. (2023). Learning local equivariant representations for large-scale atomistic dynamics. Nat. Commun. 14, 579. <https://doi.org/10.1038/s41467-023-36329-y>.
240. Anderson, B., Hy, T.-S., and Kondor, R. (2019). Cormorant: covariant molecular neural networks. Adv. Neural Inf. Process. Syst. 32, 1–16. <https://doi.org/10.48550/arXiv.1906.04015>.
241. Bereau, T., DiStasio, R.A., Jr., Tkatchenko, A., and von Lilienfeld, O.A. (2018). Non-covalent interactions across organic and biological subsets of chemical space: physics-based potentials parametrized from machine learning. J. Chem. Phys. 148, 241706. <https://doi.org/10.1063/1.5009502>.
242. Allen, A.E.A., Csányi, G., Ortner, C., and Csányi, G. (2021). Atomic permutationally invariant polynomials for fitting molecular force fields. Mach. Learn. Sci. Technol. 2, 025017. <https://doi.org/10.1088/2632-2153/abd51e>.
243. Fuchs, F.B., Worrall, D.E., Fischer, V., and Welling, M. (2020). SE(3)-transformers: 3d roto-translation equivariant attention networks. Adv. Neural Inf. Process. Syst. 33, 1970–1981. <https://doi.org/10.48550/arXiv.2204.02394>.
244. Liu, Z., Lin, L., Jia, Q., Cheng, Z., Jiang, Y., Guo, Y., and Ma, J. (2021). Transferable multilevel attention neural network for accurate prediction of quantum chemistry properties via multitask learning. J. Chem. Inf. Model. 61, 1066–1082. <https://doi.org/10.1021/acs.jcim.0c01224>.